Accepted Manuscript

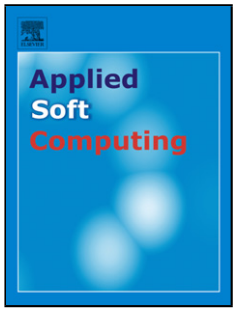

Title: An Unsupervised Learning Method with a Clustering Approach for Tumor Identification and Tissue Segmentation in Magnetic Resonance Brain Images

Author: G. Vishnuvarthanan M. Pallikonda Rajasekaran P. Subbaraj Anitha Vishnuvarthanan

PII: S1568-4946(15)00588-8
DOI: http://dx.doi.org/doi:10.1016/j.asoc.2015.09.016
Reference: ASOC 3202

To appear in: *Applied Soft Computing*

Received date: 2-3-2015
Revised date: 27-6-2015
Accepted date: 9-9-2015

Please cite this article as: G. Vishnuvarthanan, M.P. Rajasekaran, P. Subbaraj, A. Vishnuvarthanan, An Unsupervised Learning Method with a Clustering Approach for Tumor Identification and Tissue Segmentation in Magnetic Resonance Brain Images, *Applied Soft Computing Journal* (2015), http://dx.doi.org/10.1016/j.asoc.2015.09.016

List of Authors for the article entitled "An Unsupervised Learning Method with a Clustering Approach for Tumor Identification and Tissue Segmentation in Magnetic Resonance Brain Images" - ASOC_ASOC-D-15-00447

Author1: Dr. G. Vishnuvarthanan

Affiliation: Associate Professor, Department of ICE, Kalasalingam University.

Address for communication: Associate Professor, Department of ICE,
Kalasalingam University, Anand Nagar,
Krishnankoil-626 126.Srivilliputtur (Via), Virudhunagar (D.t),
India

Contact Number: +91 9360654171

Email id: gvvarthanan@gmail.com

Author2: Dr. M. Pallikonda Rajasekaran

Affiliation: Professor, Department of Electronics and Communication Engineering, Kalasalingam University.

Address for communication: Professor and Head,
Department of Electronics and Communication Engineering,
Kalasalingam University, Anand Nagar,
Krishnankoil-626 126.Srivilliputtur (Via), Virudhunagar (D.t),
India

Contact Number: +91 9443065795

Email id: mpraja80@gmail.com

Author3: Dr. P. Subbaraj,

Affiliation: V.S.B College of Engineering,

Address for communication: Principal,

V.S.B College of Engineering, NH – 67, Covai Road,

Karudayampalayam Post, Karur, Tamil Nadu 639111, India

Contact Number: +91 9443065795

Email id: subbaraj_potti@yahoo.com

Author4: Mrs. Anitha Vishnuvarthanan,

Affiliation: KLN College of Engineering,

Address for communication: M.Tech, Department of ECE,

KLN College of Engineering, Pottapalayam, Madurai (D.t), India

Contact Number: +91 994434505

Email id: anithaa06@gmail.com

Highlights for review:

1. Unsupervised neural network technique along with clustering procedure, well capable of identifying heterogeneous tumor region in multi – channeled Magnetic Resonance brain images (T1 –w, T2 – w, FLAIR and MPR sequences) is proposed.
2. Novel SOM based FKM algorithm for tissue segmentation and tumor identification is proposed through this work.
3. Exact demarcation between tumor and edema region is characterized.
4. Validation of the segmented results by an experienced radiologist.
5. Cross comparison with FCM, SOM, FKM and other hybrid clustering algorithms using ten standard comparison parameters.

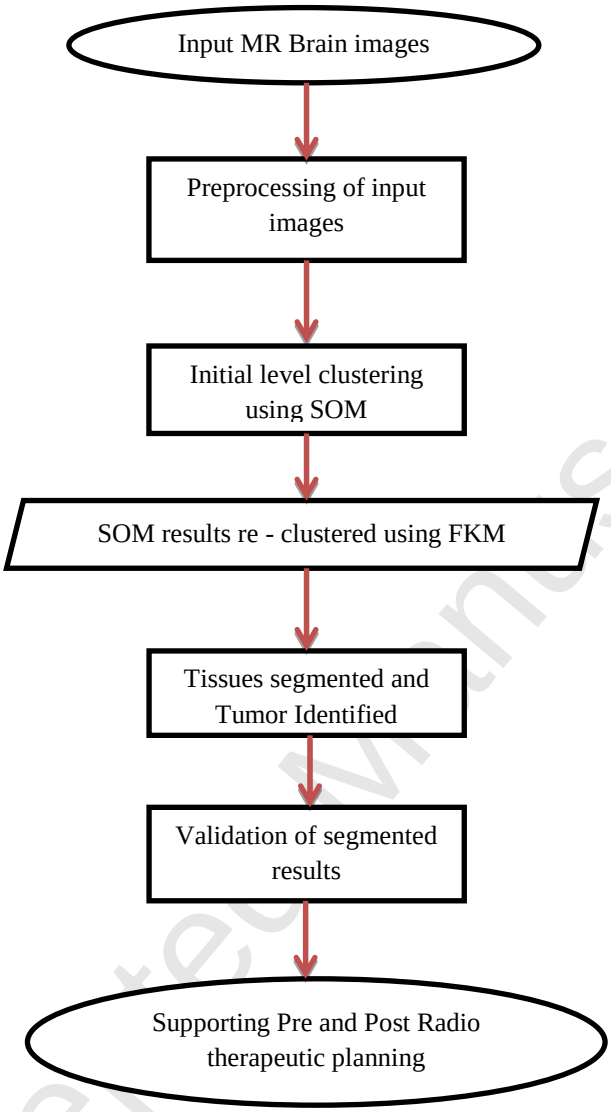

An Unsupervised Learning Method with a Clustering Approach for Tumor Identification and Tissue Segmentation in Magnetic Resonance Brain Images

Abstract:

Malignant and benign types of tumor infiltrated in human brain are diagnosed with the help of an MRI scanner. With the slice images obtained using an MRI scanner, certain image processing techniques are utilized to have a clear anatomy of brain tissues. One such image processing technique is hybrid Self Organizing Map (SOM) with Fuzzy K Means (FKM) algorithm, which offers successful identification of tumor and good segmentation of tissue regions present inside the tissues of brain. The proposed algorithm is efficient in terms of Jaccard Index, Dice Overlap Index (DOI), Sensitivity, Specificity, Peak Signal to Noise Ratio (PSNR), Mean Square Error (MSE), computational time and memory requirement. The algorithm proposed through this paper has better data handling capacities and it also performs efficient processing upon the input Magnetic Resonance (MR) brain images. Automatic detection of tumor region in MR (Magnetic Resonance) brain images has a high impact in helping the radio surgeons assess the size of the tumor present inside the tissues of brain and it also supports in identifying the exact topographical location of tumor region. The proposed hybrid SOM – FKM algorithm assists the radio surgeon by providing an automated tissue segmentation and tumor identification, thus enhancing radio therapeutic procedures. The efficiency of the proposed technique is verified using the clinical images obtained from four patients, along with the images taken from Harvard brain repository.

Keywords:

SOM (Self Organizing Map), FKM (Fuzzy K – Means algorithm), MR brain Tumor Identification, Tissue Segmentation, Peak Signal to Noise Ratio (PSNR), Jaccard Index, Dice Overlap Index (DOI), Sensitivity, Specificity, Mean Square Error (MSE) and Computational time.

1. Introduction:

An image is composed of several groups of pixels or voxels. Segmentation is an image processing technique, in which different regions of an image are segregated based upon the pixel intensities available within the image. Boundary and edge-based segmentation are the two types of segmentation procedure, of which, boundary based segmentation is used extensively **[61]**.

Magnetic Resonance Imaging (MRI) helps in obtaining a structural three dimensional image of the internal parts of human body. It, based on the principle of Nuclear Magnetic Resonance (NMR), provides a better augmentation in analysing heart, lungs, pelvis, abdomen and soft tissues in brain. The principle of NMR is as follows. Our human body is made of 80% hydrogen atoms. Hydrogen atom has a strong positive nucleus comprising proton particle. This proton has its own spin velocity, spin direction and axis of rotation. The parallel alignment of the hydrogen nuclei is set by a super conducting magnet cooled with helium liquid. The hydrogen nuclei, at this state, are subjected towards a radio frequency radiation. It

disturbs the analogous alignment of the hydrogen nuclei. As the nuclei absorb some quantity of radio frequency signal, they shift from lower energy level state to higher energy level state. As soon as the radio frequency radiation is stopped the nuclei get back to their original position with some emission of relative energy. This emitted energy, from the shifting of nuclei from excited state of energy to ground state, is recorded and processed by using a signal processor. This procedure gives out a spatial image of the internal structure of human body. The same procedure is used repeatedly to obtain 3D MR brain images. In an MRI scanner two dimensional Fourier transform is done upon the obtained image structures. On these obtained MRI images, segmentation is done by using SOM based FKM for unique tumor identification and tissue segmentation.

Cancer cells play a major role in tumor formation inside the human body. A survey made by Times of India has identified that nearly 3 million people living in India suffer from cancer, out of which 1 million people are registered with new forms of cancer. The effects created by tumor are extremely pervasive, leading to the formation of lesions and tumor within the human body. The most complicated organ of our human body is the brain. Cancer cells affecting the tissues of brain stimulate tumor formation. Though manual segmentation of brain tissues and identification of tumor region is available, an automated algorithm capable of both tumor identification and tissue segmentation processes is proposed through this paper.

Conventional analysis of MR brain images preferred by a medical expert is quite a complicated and time consuming task. The accuracy of diagnosis entirely relies upon the experience possessed by the expert. Manual procedures involving tumor identification and tissue segmentation are prone to error and inaccuracy, where noises or interferences produced by the magnetic field and radio frequency signals occupy a predominant position. So, it is inevitable to have an automatic segmentation technique to offer considerable results.

Some of the MR (Magnetic Resonance) brain image sequences are classified as T1, T2, FLAIR (Fluid Attenuated Inversion Recovery) and MRS (Magnetic Resonance Spectroscopy) images. T1 weighted images depict white matter as white in color (inner tissue region) and grey matter (outer tissue region) as grey in color, whereas, it is white color for grey matter and grey color for white matter in case of T2 weighted images. FLAIR images support the radiologist in viewing the tissues of the brain in a better perspective by suppressing the fluid content (Water and Cerebrospinal fluid) in brain. T1, T2 and FLAIR image sequences are segmented by the proposed SOM – FKM algorithm.

Nandha Gopal **[1]** referred an automatic detection of brain tumor, capable of producing an accuracy of 95.16% in segmenting MR (Magnetic Resonance) brain images, that requires further improvement.

Govindaraj Vishnuvarthanan and Murugan Pallikonda Rajasekeran **[2]** suggested an automated tumor extraction and tissue segmentation using basic Fuzzy Inference System. It has shortcomings in terms of computational time, PSNR and MSE.

El-Hachemi Guerrout *et al* **[3]** used Markov Random Field Theory for medical image segmentation. The algorithm performs medical image segmentation on a Cluster of PCs using Markov Random Field Theory. Segmentation process is done only upon T1 and contrast enhanced T1 weighted images.

2. Related Work:

Ben George and Karnan **[4]** attempted to produce segmentation results of MR brain images in a computational time of 31.21 seconds using Bacteria Foraging Optimization technique. Computational time of an algorithm plays a major role in the process of diagnosing. Lesser computational time supports the radiologist to segment large volumes of clinical data. Sultan Aljahdali et al **[5]** suggested an automated fuzzy rule based algorithms for reliable image segmentation. T1 weighted images were segmented using both fuzzy K means and Kernel based Fuzzy C Means (FCM) algorithms. Time consumption plays a major constraint in segmenting the images. Sultan Aljahdali and Zanaty **[6]** proposed an automated image segmentation using modified fuzzy algorithms, where improvement of segmentation accuracy and computational speed remains inevitable in the case of medical image segmentation. Somasundaram and Kalaiselvi **[7]** recommended a complete automated brain extraction algorithm for axial T2 weighted images. Other modalities of MR brain image sequences could be discussed too. Vasuda and Satheesh **[8]** introduced an improved FCM algorithm for MR (Magnetic Resonance) brain image segmentation. Reduction of convergence rate of the proposed algorithm remains a major setback. Logeswari and Karnan **[9]** reported brain tumor detection using a segmentation process based on Self Organizing Maps (SOM). The segmentation process is curbed to segment T2 weighted image sequences. Logeswari and Karnan **[10]** offered a brain tumor detection using segmentation process based on Hierarchical Self Organizing Map (HSOM) technique, where T2 weighted images were segmented in an average time period of 29.9708 seconds, which requires further minimization. Artem Mikheev et al **[12]** have recommended a segmentation algorithm which works only in segmenting high resolute T1 weighted images using techniques such as thresholding, surface detection, connectivity and a novel constrained growing operator. Yan Li and Zheru Chi **[13]** performed MR brain image segmentation using SOM, which requires reduction in MSE values. Andac Hamamci et al **[16]** introduced a novel segmentation algorithm only for segmenting Contrast Enhanced T1 weighted images. Meritxell Bach Cuadra et al **[17]** initiated a semi – automated atlas based segmentation of MR images with pathologies. Vida Harati et al**[22]** has utilized Fuzzy Connectedness (FC) for segmenting and identifying tumor region only in T1 weighted images. Yu and Yang **[23]** recommended a generalized FCM (GFCM) structure to consolidate the variations found in FCM and then observed its optimality test using parameter selection. GFCM does not involve the optimality test associated with both clusters and membership functions. Rather, GFCM involved optimality test only with the cluster prototype. Yu and Yang **[24]** recorded a substitutional method for GFCM and named it as Generalized Fuzzy Clustering Regularization (GFCR). GFCR is associated with the optimality test done using membership functions. Shen et al **[25]** projected a novel FCM algorithm, named Improved FCM (IFCM). Two important parameters that address neighborhood pixel attraction are suggested through this work. The first

parameter is concerned with the feature difference between neighbouring pixels present in the image and the second parameter is the link towards the calculation of relative location of the neighboring pixels. This methodology performs segmentation based upon the neighbouring pixel's intensities and their specific locations. Choosing optimum parameters still remain as tedious procedures, since it paves the way for inaccuracies in image segmentation and stands to be a major hindrance in utilizing IFCM for real time applications. Moreover, IFCM requires an Artificial Neural Network (ANN) for computing these two parameters. Designing ANN and assigning the control parameters using ANN is a complicated process and results in higher time consumption for execution. Inappropriate selection of control parameters leads to improper image partitioning and the effort taken to offer effective image segmentation proves to be futile. Statistical classifiers use preset learning rules to group the voxels present in the input image. It accomplishes clustering techniques which classify voxels in an unsupervised mode, by which similar voxels are grouped into the same class. A similarity protocol is to be extensively studied to analyze the grouping of voxels into a class. As said by Riad et al **[26],** classifiers are capable of generating different classes in which group of voxels with the same properties are held together. Certain statistical classifiers rely on algorithms such as expectation-maximization algorithms (EM) **[27, 28, 29]**, maximum likelihood (ML) estimation **[30]** or Markov random fields **[31, 32]**. K-means and Fuzzy k-means are widely used in the field of image segmentation as they avoid abrupt transferences during the classification process **[33]**. Generalization property exhibited by the support vector classifiers **[34]** has favored its utilization in the domain of image segmentation. Functioning of these classifiers is governed by statistical learning theory **[35].** Some other segmentation techniques are developed using ANN classifiers **[36 to 42]**, such as self-organizing maps (SOM) **[38 to 41, 43].** In presence of several image segmentation procedurals, no one technique is available to segment heterogeneous tumor region present in different sequences of MR brain image. Almost all the above mentioned algorithms provide proper MR brain image segmentation with the absence of efficient partition between tumor region and edema portion. With this motivation, a novel technique combining the working principles of SOM and FKM algorithms is proposed through this work. Also, different tumor sizes could be identified with the proposed methodology. This technique almost satisfies the needs of a radio surgeon and is up to the mark in assessing aberrant regions. The only limitation of the proposed methodology is that the tumor regions in an input image with extreme intensity variations cannot be clearly visualized. Further benefits of the proposed algorithm are clearly enumerated in Section 3.

2.1 Medical Image Treatment:

Digital image processing has impacted medical images by offering enhanced vision, through which better diagnosis and treatment can be emphasized **[40, 61]**. Some of the elegant usage of medical image processing has paved the way for epitomized therapeutic procedures. Normally, medical images are capable of revealing the internal anatomy of human body, where, assessment and enhancement of so said medical images are made available with the support of image processing techniques. Some other applications of medical image processing **[61]** are mentioned below for better understanding.

1) Amendment of densities present in the dynamic range of black and white images.
2) Rectification and alteration of colors in color images.
3) Aberrant region detection using Contours.
4) Calculation of cell area in a biomedical image.
5) Restoration and smoothing of images.
6) Multiple image registration and mosaicking.
7) Constructing 3-D images from 2-D images.
8) Generation of negative images.
9) Zooming of images to visualize specific targets.
10) Pseudo coloring or artificial coloring.
11) Measurements in point to point basis.
12) Removal of artifacts and noise signals present in the image.

2.2 Fuzzy Logic Clustering:

Clustering is a widely used mathematical procedure which performs segmentation process to identify the structures and irregular shapes present in an input image or dataset **[60, 61]**. Fuzzy based clustering helps partition an input image into several homogenous classes or clusters, by which identical terms are grouped in a same class and non-identical items belong to different classes. Several parameters are used to evaluate the similarity and dissimilarity of classes. Some such parameters are distance calculation, connectivity, centroid, density and intensity. Further, clustering can be differentiated into two main processes, namely soft clustering and hard clustering. Hard clustering is just like any ordinary clustering wherein the input image is partitioned into clusters and the data items (pixels) of the image should lie within the prescribed clusters. In other words, the pixels are confined to specific clusters **[61]**. In the case of fuzzy mixed clustering, pixels or data items can lie in one or more clusters. The pixels are provided independence in fuzzy based clustering techniques. The clusters are related to fuzzy technique using membership function or degree of coincidence (similar resemblance). Fuzzy based clustering has been extensively used in the domains of data analysis, pattern recognition and image segmentation.

$$A = \begin{bmatrix} a_{11} & \dots & a_{1N} \\ \vdots & \ddots & \vdots \\ a_{n1} & \dots & a_{nN} \end{bmatrix} \qquad (1)$$

As per Equation 1, $a_k = \{a_{1k}, \dots \dots \dots a_{nk}\}^T$. Here, each data set (or) pixels comprise of n measured variables which is classified as an n – dimensional column vector a_k. Normally, $a_k \in R_n$. The total number of observations is depicted as Z, where $Z = \{a_k | k = 1, 2, 3 \dots N|\}$. Z is usually represented as an $n \times N$ matrix **[60, 61]**. This is how fuzzy based clustering is generally implemented and the same has been extended to this research work.

2.3 Neural Networks:

Neural Networks are formulated using the functionality exhibited by the biological nervous systems, especially the human brain. Artificial Neural Network (ANN) acts as an information processing system and it comprises of large number of interlinked neurons for processing the input information. The working of these neurons takes place in a combined fashion and they later get distributed to perform the learning of the input information. The neurons control the internal working operation and finally derive out an optimized result. Several neural network algorithms dealing with medical image analysis, specifically about image segmentation have been explained in section 2. Computer aided diagnosis is extremely favoured by neural network, as it possesses the character of adaptive learning from input information. Further, with a suitable artificial machine learning algorithm, a wide range of inputs with severe variation could be easily assessed **[57, 61]**. Moreover, optimizing the relationship between inputs and outputs is accomplished by ANN. Speculative results for medical image visualization to enhance the diagnosing procedures are made available with the support of Artificial Neural Network (ANN) techniques.

3. Scope of our work:

The main aim of our methodology is to offer an automated hybrid algorithm to identify the tumor region present in the brain images. An automated algorithm greatly assists the radio surgeon in the process of non – invasive diagnosis of the patients affected with tumor. Further, image sequences of an MRI scanner with all the three axes namely, coronal, sagittal and axial are segmented with the support of the proposed algorithm. Levels of tumor infiltration are clearly analysed with the help of the proposed methodology. A radio surgeon can efficiently plan for pre and post radio therapeutic procedures using the hybrid SOM – FKM algorithm. Comparison parameters validate the performance of the algorithm and the results are compared with Fuzzy C Means (FCM) algorithm. Since, FCM and FKM are the two standard competitive clustering algorithms, we choose FCM as an algorithm to compare with FKM combined with SOM strategy. This paper is organized by explaining the materials and methods in section 4, which is further subdivided in explaining the functionary of FCM, FKM, SOM and the combination of SOM and FKM in sections 4.1, 4.2, 4.3 and 4.4 respectively. Details of input images used in the algorithm are explained in section 4. Section 5 explicates the comparison parameters chosen for evaluating the proposed technique. Section 6 briefs the results obtained using SOM based FKM technique. Finally, section 7 gives out the conclusion. Section 4 also briefs the adopted initial level pre-processing procedures. SOM is chosen to offer initial level clustering to enhance the performance of FKM algorithm, as K – means in FKM is generally a greedy algorithm which provides faster convergence with minimal efficiency **[15]**. To overcome this hindrance in FKM, SOM is used and moreover, such a combination of algorithms does not exist. This has been a stimulant to develop SOM based FKM algorithm for medical image segmentation, so as to effectively analyse the cancerous regions.

4. Materials and Methods:

A simple flowchart explaining the sequential steps of the proposed method is given in **Fig. 1** for easy understanding. Following the flow diagram in **Fig.1**, an initial level pre-processing is done to remove the skull region from the given input images. The images have been obtained using a Siemens – Aera 1.5 T Magnetom Avanto-Tim technologies equipped MRI scanner of 1.5 T magnetic field intensity. The total number of channels required to capture the image is around 48. The scan parameters used for attaining the MR images are: FLAIR: SL/TE/TR/TI – 5/82/8000/2500, T1 – w: SL/TR/TE – 4/10/550 and T2 – w: SL/TR/TE – 5/117/4000. Here, scan parameters SL, TR, TE and TI denote settling time, relaxation time, spin echo time and inversion sequence time, respectively. The total time duration for acquiring the images is found to be less than 10 min. The slice thickness of the MR brain images obtained from four patients suffering from different types of lesions is found to be 1mm×1mm×1mm. Removal of skull region is inhibited using Brain Extraction Tool (BET) as specified in **[48]**. Segmentation of tissue region and identification of tumor region are the main concerns of this research and the above said factors have compelled to use BET and ROI (Region of Interest) based brain masking for initial level image processing. BET **[7, 48, 58]** and ROI are the conventional techniques used extensively for skull stripping. These techniques favour the user to choose the region of upmost interest (brain tissues) and also to eliminate the regions of least priori, which are performed through manual interaction. Also, images from Harvard Brain Repository have been used to validate the proficiency of the proposed algorithm. Normally, images acquired through an MRI scanner are 3D in structure (mixture of axes namely: Coronal, Sagittal and Axial) and image segmentation is performed on individual 2D slices of the 3D structures **[19]**. This main property is inhibited by the proposed SOM based FKM algorithm. T1, T2 and FLAIR may be one among the 2D slice image, upon which the segmentation steps are implemented.

4.1 Fuzzy C Means Algorithm (FCM):

Fuzzy C - means (FCM) algorithm is a clustering methodology introduced by Dunn, enhanced by Bezdek and further titivated by Matteo Matteucci and it groups the voxels (data) of the Magnetic Resonance (MR) brain images as *'n'* number of clusters. The neighbouring pixel of least mean distance from the centroid pixel are assigned with low membership grade value and are grown around the centroid value, hierarchically **[49]**. The membership grade and the cluster centres are iteratively updated to reduce the objective function of grouping the voxels.

$$J_k = \sum_{i=1}^{N} \sum_{j=1}^{C} \delta_{ij} \left\| x_i - c_j \right\|^2 \qquad (2)$$

N describes the number of data points given as an input to the algorithm (Total number of voxels or voxels present in the image). *K* illustrates the number of iterations to be performed. C = $\overrightarrow{x_i}(t+1)$ states the number of clusters into which the voxels are to be grouped. c_j denotes the centre vector for the clusters (Centroid value of the voxels). x_i defines the data points (voxels). δ_{ij} is the degree of membership for the i^{th} data point of x_i in cluster j. $\left\| x_i - c_j \right\|$ refers the measuring the similarity or mean distance of the neighbouring voxels present in the data point x_i to the centre vector (centroid value) of cluster j.

Degree of membership is given as, $\delta_{ij} = \frac{1}{\sum_{k=1}^{C}\left(\frac{\|x_i - c_j\|}{\|x_i - c_k\|}\right)^{\frac{2}{m-1}}}$ (3)

m = Fuzziness co – efficient obtained from the overlapping of clusters and it is defined as $1.5 \leq m \leq 2.5$ for optimum segmentation results **[18]**. c_k is the centroid value for '*K*' iteration. Centre vector (Centroid voxel) for the cluster is defined as,

$$c_j = \frac{\sum_{i=1}^{N} \delta_{ij} * x_i}{\sum_{i=1}^{N} \delta_{ij}} \quad (4)$$

During the initial processing of the algorithm, $\delta_{ij} = \theta_{ij}$. Where, θ_{ij} is a random value initialized as, $0 \leq \theta_{ij} \leq 1$(Usually expressed as 0, 0.1, 0.2, 0.4….1), such that, $\sum_j^C \delta_{ij} = 1$.

In general, FCM algorithm has greater data handling capacity and has better operability upon diversified data range. On the other hand, the convergence rate gets affected if the number of clusters and iterations are subsequently increased. Diminishing the number of iterations and clusters to obtain faster convergence rate has an adverse effect upon the segmentation accuracy. To overcome these hindrances, a novel segmentation algorithm which combines SOM and FKM is proposed through this paper.

4.2 Fuzzy K Means algorithm (FKM):

Fuzzy K means algorithm, also called FKM, acts a stiff competitor to FCM algorithm. As mentioned by Chih-Tang Chang et al **[15]**, FKM partitions the given input image into '*k*' clusters (partitioning the voxels present in the image).

$$J = \sum_{j=1}^{K} \sum_{i=1}^{N} u_{i,j}^{m} d_{ij} \quad (5)$$

Here, *N* represents the number of data points or voxels present in the input MR brain image. *K* refers to the number of clusters formed by FKM. i j explain the rows and columns of the input image. $u_{i,j}^{m}$ defines the membership functions of FKM with fuzziness coefficient m (fuzziness co – efficient is obtained from the overlapping of clusters). d_{ij} is the squared Euclidean distance between pixel X_i and cluster representative C_j (Cluster center or centroid value). FKM algorithm has quicker convergence rate and requires less computational time for processing an image. It has limitations in handling the data of wider range. Taking favour of quicker convergence rate, FKM is used in the proposed methodology and the problem of data range handling is overcome using SOM.

4.3 Self Organizing Map Algorithm:

The first step of processing an SOM algorithm commences with initialization, where voxel intensities are initially assessed and modelled with the assistance of SOM prototypes. This process is executed using histogram analysis, which acts as a replacement for mixtures

of probability density functions. Histogram based model helps analyse the peaks and valleys of the input image and further supports in sustaining unique informative values of voxel, which can be greatly used in segmentation process **[14, 19, 47]**. Over fitting is a severe issue which occurs due to redundancies of data and it requires immediate attention. The issues of over-fitting and model selection in self-organizing map are resolved with the help of histogram, mean and variance values **[59]**. Histogram helps in assigning the nearest prototype value to the voxels present in the image, ultimately providing models to SOM, whereas, K-means clustering (number of clusters =3) is used by Ortiz et al **[19]** for modelling the inputs to SOM. Interpolation of mean and variance values helps in the suppression of redundancies **[19, 59]**, by which over fitting in SOM could be reduced considerably. The SOM algorithm is explained as follows:

Let $X \in R^d$, where R^d represents the diversified input data and X is the input vector. The winning unit is calculated in each iterative step as,

$$U_\omega(t) = argmin_i\{\|x(t) - \omega_i(t)\|\} \quad (6)$$

$x \in X$, where $x(t)$ is defined as the input vector at time instant '*t*' and $\omega_i(t)$ is the sample vector related to the unit '*i*'. The unit quite closer to the input vector $U_\omega(t)$ is denoted as winning unit and the associated prototype or the sample vector is sequentially updated **[19, 56]**. The adaptive learning process in SOM is completed by updating the prototypes of the units in the neighborhood of the winning unit. This procedure is described as,

$$\omega_i(t+1) = \omega_i(t) + \propto(t) h_{Ui}(t)(x(t) - \omega_i(t)) \quad (7)$$

Here $\propto(t)$ is the exponential decay learning factor and $h_{Ui}(t)$ is the neighborhood function related to the unit '*i*'. Both learning factor and the neighborhood function decrease with respect to time and the adaptability of prototypes becomes slower as the neighborhood of the unit '*i*' contains few units **[19, 55]**.

$$h_{Ui}(t) = e^{\left(-(\|r_u - r_i\|^2 / 2\sigma(t)^2)\right)} \quad (8)$$

Equation 8 explains the neighborhood function, where r_i denotes the position on the output space and $\|r_u - r_i\|$ is the distance between the winning unit and the unit '*i*' on the output space. The neighborhood function is explicated using a Gaussian function, which consistently shrinks on completion of every iteration step and is briefed in Equation 9. The winning unit found during this process is called the Best Matching Unit (BMU) **[19, 55, 56]**. Consecutively, $\sigma(t)$ controls the reduction of the Gaussian neighborhood in each iteration step using the time constant τ_1.

$$\sigma(t) = \sigma_0 e^{(-t/\tau_1)} \quad (9)$$

The prototype ω_i present in SOM acts as the centroid of a Voronoi polyhedron **[19, 55]**. SOM is capable of projecting the prototypes either in two dimensional or three dimensional spaces. This representation occurs based on the dimension of the output layer. Initial level grouping of the prototypes is done using SOM. Prototypes which are quite similar in nature are placed closer to the output space. This placement of prototypes is usually performed based on Euclidean distance calculation. The location of the prototypes on the output space tends to be a valuable source of information and can be utilized to cluster the SOM **[19, 45]**. Based on the eigenvalues and eigenvectors of the training data, linear initialization of the SOM prototypes is performed. The prototypes are sorted in the form of hexagonal lattices. This process is performed based on the width of the lattice and its proportionality towards the standard deviation of the first principal component **[19, 44, 47]**. This indicates the arrangement of the prototypes: the first dimension of the prototypes is aligned proportionally to the first principal component and the second dimension of the prototypes is aligned proportionally to the second principal component. On complete estimation of the optimal number of map units, the unsupervised neural network is nearly trained. The above mentioned calculations are executed during the initialization of SOM map. On completion of the map initialization process, feature vectors obtained from the normalized dimensionality confined feature space developed for zero mean and unity variance is used to train the unsupervised neural network. This procedure can also be called data whitening. Normalization of the feature vectors used for training the map supports in reducing the influence of one dimensional value, which occurs due to the extracted features of variable property **[19, 59]**. As an outcome of the adopted training procedurals, a group of prototypes assembled on the SOM layer supports in modeling the features of the volume image histogram. A unique classification process is performed based on assigning the closest prototype for each voxel. Exact depiction of the data is accomplished with the aid of the prototypes obtained during the training process, which indicates the quality of the SOM technique. The effectiveness of the trained map is ascertained using the following conditions (i) generalization of the input data using the prototypes and (ii) distance evaluation between the similar prototypes present in output space or in other words it is the denotation of topology preservation **[19, 56]**.

Quantization error (t_e) and the topological error (q_e) are the two important quality assessment parameters for the trained map. Quantization error (t_e) is related to the measurement of average distance between the individual data vector and the Best Matching Unit (BMU). Topological error (q_e) defines the measurement of data vectors proportionality, for which the first and second Best Matching Unit (BMUS) are non – adjacent **[19]**. Quantization error and the topological error are described in Equations (10) and (11).

$$t_e = \frac{1}{N}\sum_{i=1}^{N} u\,(\vec{x}_i) \qquad (10)$$

$$q_e = \sum_{i=1}^{N} \left\| \vec{x}_i - \vec{b}_{\vec{\omega}_i} \right\| \qquad (11)$$

In Equation (10), N denotes the total data vectors; $u(\vec{x}_i)$ = 1 if non – adjacency is preserved by first and second BMU for $(\vec{x}_i)$, or else $u(\vec{x}_i)$ = 0. In Equation (11), $\vec{b}_{\vec{\omega}_i}$ represents weight function related to the BMU of data vector $\vec{x}_i$, where $\vec{x}_i$ is the i^{th} data vector present in the input space and is capable of defining the quantization error. Hence, lower quantization error (t_e) and topological error (q_e) affirm better data representation and topological preservation and therefore provide better clustering result. Betterment of SOM algorithm is coined by lower quantization error and topological error **[19, 46, 47]**.

Here, SOM itself is an unsupervised neural network based clustering technique, which can be directly used in segmentation process **[9, 19]**.

4.4 Proposed methodology:

The combination of SOM and FKM is the main novelty proposed in this paper. SOM is used for initial clustering and it offers dimensionality reduction **[19]**. The image given as input to the algorithm is of varied dimensions, which is reduced with the aid of SOM algorithm and displayed as a two-dimensional map. The size of the map is 8 × 8. Prototype ω_i, **[14]** is the resultant value obtained using SOM. The classified prototypes obtained using SOM is given as the inputs to FKM algorithm. Thus the problem aroused due to FKM in handling wide and large data range is minimized with the inclusion of SOM. Next, FKM utilizes the output from SOM and performs the clustering operation as specified in **[15].** Prototype ω_i is the input fed to FKM algorithm and the following process takes place sequentially:

$$J_K = \sum_{j=1}^{k} \sum_{i=1}^{N} u_{i,j}^{m} d_{ij} \qquad (12)$$

Here, K describes the total number of iterations. U_{ij} represents the membership function and its calculation is described in equation (13). d_{ij} represents the Euclidean distance calculation.

$$U_{ij} = [\,(d_{ij})^{\frac{1}{m-1}} \sum_{l=1}^{K} \left(\frac{1}{d_{ij}}\right)^{\frac{1}{m-1}}\,]^{-1} \quad (13)$$

Here, $d_{ij} = \|x_i - c_j\|^2$. 'm' denotes the fuzziness co – efficient obtained due to the overlapping of clusters. 'm' is entered as 2.0 as it gives out optimal segmentation results and is derived from **[18]**. *'k'* denotes the number of clusters into which the prototype ω_i is to be partitioned. *l = 1* represents the first cluster. 'x_i' is the location of the data x at the i^{th} position and it belongs to the prototype ω_i. This specific task has been motivated from **[55, 56]**.

- High membership function is assigned to the data point which lies very near to the cluster centre.
- In Equation (14), C_j denotes the cluster center. C_j can also be called cluster representative.

$$C_j = \frac{\sum_{i=1}^{N} U_{ij}^m X_i}{\sum_{i=1}^{N} U_{ij}^m} \qquad (14)$$

- Equation (15) explicates the sum function of membership values of each data point and it should be equal to one.

$$\sum_{j=1}^{k} U_{ij} = 1, \text{ for } i = 1 \text{ to } N \qquad (15)$$

Function J_K, explains the final segmentation result attained from FKM algorithm. As a whole, SOM has greatly supported FKM algorithm by offering an initial level segmentation.

The efficiency of the proposed methodology is explained using comparison parameters and is briefed in results and discussions. Clinical and live images of patients suffering from High grade Astrocytoma, Glioma, Primitive Neuro Ectodermal, Meningioma, Nerve sheath and Metastatic Bronchogenic Carcinoma tumors are fed as input to the proposed methodology.

5. Comparison Parameters:

5.1 MSE (Mean Square Error):

Mean Square Error defines the process of squaring the differentiated quantities **[20, 49]**. It is expressed as the average of the squares of the errors obtained by subtracting the input and the output values. MSE is the cumulative squared error value between the input image $A(i,j)$ and the segmented image $B(i,j)$.

$$MSE\ (Mean\ Square\ Error) = \frac{1}{mn}\sum_{i=0}^{m-1}\sum_{j=0}^{n-1}[A(i,j) - B(i,j)]^2 \quad (16)$$

'm' & 'n' denote the number of rows and columns present in an input image.

$i = m$, to perform incremental operation for 'rows' in a 'for' loop statement.

$j = n$, to perform incremental operation for 'columns' in a 'for' loop statement.

MSE value of the resulting segmented image should be as low as possible. Reduced MSE values offer minimized error occurrence in the segmented MR brain images.

5.2 PSNR (Peak Signal to Noise Ratio):

Peak Signal to Noise Ratio refers to the immunity of an image to noise signals **[21, 49]**. If the PSNR value is high, then the impact of noise interference signal upon the MR brain image is quite low. The highest pixel value of the input MR brain image is represented as MAX_I (Say 255). PSNR is expressed with the help of MSE values. The algorithm producing PSNR values ranging between 40 to 100 dB is considered to be less sensitive to noise signals. Segmented results obtained with high PSNR values can be used in image compression procedures for image storage and image transmission through the internet facilities. PSNR depicts resistance to the noise signals and also briefs the quality of the segmented image. PSNR is usually expressed as:

$$PSNR = 10\,log_{10}\left(\frac{MAX_I^2}{MSE}\right) = 20\,log_{10}\left(\frac{MAX_I}{\sqrt{MSE}}\right) = 20\,log_{10}(MAX_I) - 10\,log_{10}MSE \quad (17)$$

5.3 Memory Requirement:

The memory space required by the combinational algorithm to perform the segmentation process is described in terms of memory requirement. The memory required for an image segmentation process should be minimal. Lower memory requirement proves the efficacy of the segmentation algorithm and is expressed in bytes.

5.4 Computational Time:

The time required for the accomplishment of segmentation process is denoted in terms of seconds. The proposed SOM - FKM consumes lesser time when compared with FCM algorithm.

5.5 Jaccard (Tanimoto) Index:

Jaccard index is denoted as the ratio of the common voxels present in the input image (*A*) and the segmented output image (*B*) to the union function or the collection of voxels present in the input image (*A*) and the segmented output image (*B*) **[16, 49]**. In other words, it is the ratio between the intersection and the union functions of the voxel values present in the input image (*A*) and the segmented resulting image (*B*).

$$J(A,B) = \frac{S(A \cap B)}{S(A \cup B)} \quad (18)$$

5.6 Dice Overlap Index (DOI):

DOI value is expressed with the aid of Jaccard index *J (A, B)*. DOI defines the overlapping function of the input image (*A*) and the segmented output image (*B*) **[16, 49]**.

$$D(A,B) = 2 \times \frac{J(A,B)}{1+J(A,B)} \quad (19)$$

5.7 Similarity Index (SI):

Similarity Index describes the similar or identical values between the input image (*A*) and the segmented output image (*B*) **[11, 49]**. It relates to the similarity found between the input image and the final segmented image which comprises detected tumor region along with the identification of tissue regions. The values used to calculate SI are:

1. True Positive (*TP*): Exact classification of tissue region and identification of tumor region.
2. False Positive (*FP*): Misidentification or misclassification of normal tissue region as tumor region.
3. False Negative (*FN*): Tumor region undetected or misclassified.

$$SI = \frac{2 \times TP}{2 \times TP + FP + FN} \quad (20)$$

5.8 Overlap Fraction (OF) or Sensitivity:

Overlap Fraction (*OF*) or sensitivity value refers to the proper segmentation or classification of the input image **[11, 49]**. Moreover, OF defines the success rate in exact identification of tumor region and other tissue regions. It is stated as:

$$OF = \frac{TP}{TP+FN} \qquad (21)$$

5.9 Extra Fraction (EF):

Extra Fraction (*EF*) mentions the number of voxels falsely detected as tumor region. In addition, the misclassification rate of tissue regions too is taken into account **[11, 49]**. The algorithm which is capable of producing lower EF value offers better segmentation results. EF is described as:

$$EF = \frac{FP}{TP+FN} \qquad (22)$$

5.10 Specificity:

The term specificity defines the capability of an algorithm to classify or segment the normal tissue regions present in the input image **[18, 49]**. Alternatively, specificity can be defined as the exactness of an algorithm to segment the regions other than tumor region. Specificity is reckoned using Equation 23.

$$\text{specificity } (\sigma) = \frac{TN}{TN+FP} \qquad (23)$$

Here, *TN* is the True Negative value. It briefs the effective segmentation of non – tumor region or normal brain tissues by the algorithm.

5.11 Accuracy:

Accuracy, also called segmentation accuracy, is an evaluation parameter used to assess the efficacy of the segementation algorithm **[1]**. Usually, segmentation accuracy is represented as the ratio of number of pixels segmented or processed by the algorithm to the total number of pixels actually present in the input image. Segmentation accuracy is denoted in Equation 24.

$$Accuracy = \left(\frac{k}{m \times n}\right) \times 100 \qquad (24)$$

Here, *'k'* is the total number of pixels present in the segmented output image. '*m*' and '*n*' are the rows and columns present in the input image, persistently representing the total number of pixels present in the input image.

5.12 Distance Evaluation:

The proposed method infers the identification of tumor region bounded between the tissues in MR brain images. The Euclidean distance calculation for the voxels is mentioned as:

$$D_e(P, Q) = ((x - s)^2 + (y - t)^2 + (z - u))^{\frac{1}{2}} \qquad (25)$$

Here, x, y, z and s, t, u described in Equation (25) are the spatial domain values of the given input MR brain image with a Field of View (FOV) matrix value as 256 × 256. The spatial coordinate values x, y and z belong to voxel 'P'. The other spatial coordinates of voxel 'Q', say s, t and u are estimated based on the minimal distance and intensity correlation criterion. The differences and the squares of these coordinates provide (Euclidean Distance) the distance evaluation between the voxels **[60, 61]**.

6. Segmentation Results from Hybrid SOM – FKM algorithm:

Table 1 helps us to derive the average values of MSE, PSNR, TC, DOI, computational time and memory requirement. Using **Table 1**, comparison of the proposed methodology with other algorithms has been made easier.

SOM based FKM is capable of producing an average MSE value of 2.151, which is quite higher than the rival FCM algorithm, as it produces 0.0703 as the average MSE value. Even though the MSE value is little bit higher in the case of SOM based FKM algorithm, the deformation levels are quite tolerable and the segmentation results are good in nature. Comparison of MSE values is explained in **Fig. 2.**

While speaking about the size of the input images, the clinical datasets are of dimensions 480 × 375 for axial plane, 1105 × 650 for Coronal plane and 763 × 664 for sagittal plane. The axial planed images obtained from Harvard brain repository is found to be of dimension 256 × 256. Either an image compression algorithm or a segmentation algorithm should produce PSNR value ranging between 40 to 60 dB or even more. In the case of proposed segmentation methodology, 41.85 is the average PSNR value and is 18.17 dB lesser than the PSNR value produced by FCM algorithm. Since, PSNR and MSE values are inversely proportional, FCM algorithm has exceeded SOM based FKM in these terms. But, SOM based FKM has significance in producing better visualization of tumor and tissue regions. MSE and PSNR values have minimal impact upon the effeciency of the proposed methodology and they are the factors of least consideration. Jaccard **T**animoto **C**oeffecient Index (TC), usually expressed as percentage (%), gives out information regarding the similarity of voxels present in the input image and the segmented output image. The proposed SOM based FKM algorithm excels FCM by providing 31.54% as TC value, whereas, FCM produces a TC value of 21.11 %. As said earlier in section 5.5, better TC better segmentation results. Dice Overlap Index (DOI), which is quite related to TC gives out the significance of uniformity of the voxels present in input and output images. The suggested SOM – FKM algorithm is capable of producing an average DOI value of 47.36 % and FCM algorithm

produces 34.85% as average DOI value. SOM based FKM has the ability to produce better DOI values in comparison with FCM algorithm. All the above said comparisons are clearly illustrated in **Fig. 3**.

To say about memory requirement, both the soft computing methodologies were run on a 32 Bit operating system with Pentium 4 processor (2.2 GHz) and 2 GB RAM. As said in section 5.3, lower the memory space higher is the segmentation efficiency of the algorithm. The proposed algorithm has outperformed FCM in terms of memory requirement as it provides an average value of 3.24E+13 bytes. The inclusion of SOM, which acts as an initial level clustering, has impacted FKM algorithm to consume lesser memory space for its operation. FCM algorithm requires 4.48E+13 bytes for processing 38 input images. This is the advantage of the recommended SOM based FKM algorithm and it is pictured in **Fig. 4**.

The average computational time for processing 38 input MR brain images by the recommended SOM based FKM algorithm is found to be less than 2.8 seconds. On the other hand, FCM algorithm requires average time duration of 24.77 seconds for processing the input images. These explanations are clearly mentioned in **Fig. 5**.

In general, the images acquired through an MRI scanner are 3D in nature (Three dimensional) and these images are converted into 2D format (say individual slices) in order to carry out image processing operations such as segmentation, compression, reconstruction and enhancement **[19]**. The same is implemented in this research so as to segment the slices of axial, coronal and sagittal images. The proposed method has a diversified approach, as it is capable of segmenting T1, T2 and FLAIR type MR brain images. This strategy is made possible through the support of two staged clustering, of which one is offered by SOM and the other is offered by FKM.

Gold standard or the manually segmented images **[18]** help in assessing the proficiency of the proposed methodology. These images are obtained by the manual intervention offered by an expert radiologist, who has gained deep knowledge in diagnosis as an outcome of prolonged experience. Sample gold standard images are shown in **Fig. 6, 7** and **8**. These images serve as an assessment tool for analysing **Fig. 9, 16 (A)** and **18 (A)**. Due to the availability of gold standard images for both clinical and Harvard datasets, a cross comparison of SOM based FKM and FCM algorithm is performed.

Fig. 9 & 10 is obtained from the patient of age 5, suffering from PNET (Primitive Neuro Ectodermal tumor). Perfect tumor identification along with tissue segmentation is performed. Ipsilateral ventricular system is extremely compressed in the case of patient 1. T2 FLAIR Axial with Contrast Enhancement - **Fig. 9(A)**, T2 Coronary - **Fig. 9(B)** and T1 Coronary with Contrast Enhancement - **Fig. 9(C)** are obtained during the clinical diagnosis of PNET. Minimal intensity levels of Grey Matter (GM) and White Matter (WM) structures are observed in input images of **Fig. 9(B)** and **9(C),** where successive segmentation of both GM and WM is presented by the proposed SOM based FKM algorithm, which can be referred to the result part. Further, a clear cut demarcation between the tumor region and the edema

portion is visualized in **Fig. 9(A),** which proves the segmentation efficiency and robustness of the proposed algorithm.

Fig.10 is a 3D Multi Planar Reconstruction (MPR) Contrast Enhanced image of patient 1. Contrast enhancement was favoured by Gadolinium or Gado IV, a common contrasting agent which supports efficient diagnosis of the lesions and pathologies. MPR images help in analysing the anatomy of brain. A clear structure of GM and WM is visualized in the result part of **Fig. 10(A)**. Even though severe intensity variation is observed in the input image of **10(B)**, the proposed algorithm has produced a clear segmentation of GM and WM with successful detection of tumor region and can be seen in the result part of **Fig. 10(B)**. The efficacy of the proposed algorithm is literally proved in **Fig. 10**.

Fig. 11 is the complete imagery attained from the patient of age 35 suffering from meningioma. Calcified meningioma with dural tail is reported in the right parietal convexity of the brain. In **Fig. 11(A),** distinguished view upon the grooves (Gyri and Sulci) is made available and can be observed in the result part. Moreover, no clear examination of GM and WM can be done with the input images of **Fig. 11(B)** and **Fig. 11(C).** This difficulty is overcome with the help of the suggested hybrid SOM based FKM algorithm and could be verified in the result part. These challenging cases of tumor identification and tissue segmentation have been resolved with the aid of the recommended hybrid algorithm. Flair Axial **– Fig. 11(A)**, T1 Sagittal - **Fig. 11(B)** and T1 Coronary with Contrast Enhancement **- Fig. 11(C)** were used in clinical practices to diagnose the tumor region present in the meninges of brain.

After the injection of Gadolinium (or) Gado IV contrast agent and on a specific attention paid towards the right ganglio capsular region and thalamus, a heterogeneous enhancement was identified. Presence of intense edema has led to the effacement of ipsilateral ventricular system, observed during clinical diagnosis. The high grade Astrocytoma tumor region bounded between the dense edema regions is exactly detected and it is clearly visualized in **Fig. 12**. T2 Axial – **Fig. 12(A)**, T1 Sagittal – **Fig. 12(B)** and T1 Coronary with Contrast Enhancement – **Fig. 12(C)** were used to diagnose the tumor region. The above figure shows the effectiveness of the proposed methodology in resolving challenging clinical datasets where computer aided diagnosis is extensively preferred by the radio surgeon. Demarcation between tumor region and edema portions is made available in the result of **Fig. 12(A)**, and improper segmentation of tissue regions is also observable. This reduces the count of true negative value. Perfect tumor identification and tissue segmentation can be seen in the result part of **12(B)** and **12(C).** A 3D MPR with Contrast Enhancement was also used to identify the impact of high grade Astrocytoma upon the patient. The proposed hybrid algorithm succeeded in segmenting the tissue regions and has delivered perfection in tumor identification and the above said details are clearly stated in **Fig. 13**. In **Fig.13**; it is also observed that the continuous intensity variations present in the input image do not have any effect upon the working of SOM based FKM technique.

Fig. 14 & Fig. 15 were completely acquired from Patient 4 affected with supratentorial PNET and were subjected to radio therapeutic procedures. Partial identification

of tumor region is observed in **14(A).** Exact identification of tumor and segmentation of tissue regions is characterized by the proposed algorithm and it is verified in the result part of **Fig. 14(B)** and **Fig. 14(C)**. On injection of Gado IV contrast agent, a mixed enhancement was observed in the areas of right parieto-occipital lobe structures, cortical and subcortical regions. Effacement of Sulci and right lateral ventricle were visualized due to the presence of cerebral edema in larger volumes. Tumor region impinged in the dense edema portions was successfully identified and can be verified in **Fig. 14(B)** and **Fig. 14(C)**. A prominent partition between the tumor and the edema filled regions done by the proposed hybrid algorithm is illustrated in **14(C)**. T2 Axial – **Fig. 14(A)**, T1 Sagittal with Contrast Enhancement – **Fig. 14(B)** and T1 Coronal – **Fig. 14(C)** are image sequences used to diagnose the pathologies.

A 3D MPR sequence was used to examine the impact of tumor region and edema portion upon Gyri and Sulci structures. Demarcation between tumor and edema regions was exactly done with the help of SOM based FKM algorithm and it is illustrated in **Fig. 15(A)** and **Fig. 15 (B)**. Fine tumor identification made by the proposed methodology is shown in **Fig. 15(B)**.

Fig. 16 is obtained from the patients affected with low grade Glioma and metastatic bronchogenic carcinoma. T2 Axial with Contrast Enhancement - **Fig. 16(A),** is used to diagnose the malignant tumor region present in the left occipital lobe of the brain affected by low grade Glioma. T2 Axial - **Fig. 16(B)** and T1 Axial with Contrast Enhancement - **Fig. 16(C)** are the images used to diagnose the patient suffering from Metastatic Bronchogenic Carcinoma. The suggested SOM based FKM algorithm effectively segments the tumor region and is proven in the result part of **Fig. 16 (A)**, **(B)** and **(C)**. Distinguished view upon the tumor region, which is surrounded by dense edema region is made available by the proposed algorithm and is shown in **Fig.16 (A)** and **(B)**. Excellent tissue segmentation is also offered by the proposed methodology and can be visualized in **Fig. 16**.

Fig. 17, 18, 19 & **20** are Contrast Enhanced images and were attained from Harvard brain web database. These images were used to affirm the performance levels of the proposed SOM based FKM algorithm.

Fig. 17 was obtained from the patient affected with Pituitary Adenomas. T1 axial images with Contrast Enhancement offered by Gado – IV were used to diagnose the patient. The shortcoming of the proposed methodology is clearly visible in **Fig. 17(A), 17(B), 17(C)** and **17(D)**. These images also show the perfection of the proposed methodology in segmenting the tissues present in the input MR brain images. Tumor region in the above said images could not be detected and can be considered under the count of false negative.

Fig. 18 is acquired from the patient affected with nerve sheath tumors. The inefficiency of proposed algorithm related to misidentification of tumor region is shown in **Fig. 18(B).** Tissue regions present in the input images have been exactly segmented and can be verified in the result part of **Fig. 18.**

Fig. 19 states the imagery of the patient suffering from low grade Glioma. Although the images suffer from slight noise distortions caused by the radio frequency signals produced by an MRI scanner, the proposed algorithm identifies the tumor region and segments the tissue region much accurately. The proficiency of the proposed algorithm can be confirmed by viewing the result part of **Fig. 19(A), 19(B), 19(C), 19(D)** and **19(E)**.

Variable dimensions of the tumor region present in the patient suffering from high grade Glioma are perfectly identified with the support of the proposed SOM based FKM algorithm. In spite of the presence of intensity variations in the tissues of brain very near to the tumor region, the proposed algorithm successfully identifies and segments the tumor region and tissue regions respectively. The helpfulness of the proposed algorithm can be understood by looking into the segmentation results of **Fig. 20**.

The segmentation accuracy produced by the proposed SOM based FKM algorithm is 96.18% and it is quite a better accuracy level offered by the methodology recommended by Nandha Gopal **[1]**. Higher the accuracy better is the segmentation efficiency.

Fig. 21 and **Fig. 22** give a brief comparison of the segmentation results obtained from different soft computing methodologies and the proposed SOM – FKM algorithm. Column **21(A)** is the input image of patient 1 & 3 suffering from PNET and high grade Astrocytoma. As these figures are normally better segmented by the algorithms, they are presented in this paper for an effective comparison. Column **21(B)** is the segmentation result offered by Entropy based Fuzzy clustering, where tumor misidentification is observed in the first and third images. Column **21(C)** denotes the segmentation results provided by Graph based Fuzzy clustering. Good tumor identification and poor tissue segmentation is presented by this technique. Column **22(D)** explains the segmentation results derived with the aid of Kernel based Fuzzy clustering and the segmentation results attained using this technique are far better when compared with other two algorithms. **Fig. 22** describes the segmentation results acquired with the help of Self Organizing Map (SOM), Fuzzy K – Means (FKM) and SOM – FKM algorithms. It can be visualized that when SOM and FKM algorithms are executed separately, they lead to either over-segmentation or under-segmentation of the input images. To overcome these obstacles, SOM based FKM algorithm is used and the results of this algorithm can be seen in **22(D)**. Over-segmentation of FKM algorithm can be seen in the fourth image of column **22(C)** and under-segmentation of SOM algorithm can be observed in almost all the images of column **22(B)**.

Fig. 23 defines the comparison of Entropy based Fuzzy clustering, Graph based Fuzzy clustering, Kernel based Fuzzy clustering, SOM, FKM and SOM based FKM algorithms using MSE value. In producing lower MSE values, SOM based FKM ranks fourth among the traditional image segmentation algorithms.

Fig. 24 briefs the comparison of algorithms using PSNR value. As PSNR and MSE values are inversely proportional, the proposed SOM – FKM algorithm produces fourth highest PSNR value in comparison with other image segmentation algorithms.

Fig. 25 explains the comparison of Jaccard (TC) Index values. SOM based FKM produces 31.54% as the average TC value, which is quite lower than the average TC value produced by Entropy based Fuzzy clustering. As Jaccard (TC) Index values and Dice Overlap Index (DOI) values are interrelated to each other, the proposed algorithm produces an average DOI value of 47%. This value is 15% lesser than the DOI value offered by Entropy based Fuzzy clustering and it is described in **Fig. 26**.

Fig. 27 shows the comparison of average time duration required by a Pentium processor for performing MR brain image segmentation. Graph based Fuzzy clustering requires more than a minute to complete the segmentation procedure and this time duration is the highest among other algorithms. SOM requires less than 1.5 seconds to perform the segmentation process and FKM algorithm requires 2.39 seconds to produce the segmentation results. Since, SOM based FKM algorithm combines the working strategies of both SOM and FKM algorithms, it requires average time duration of 2.716 seconds.

The memory occupied by the proposed SOM based FKM is quite low when compared to SOM and FKM algorithms. It is a mediocre in consuming memory levels and can be verified in **Fig. 28**. Thus, **Figures 21 and 22** iteratively prove that the proposed SOM based FKM algorithm is far better than the contemporary algorithms in producing good medical image segmentation results, even though slight deterioration in comparison parameter values is observed. The efficacy of the proposed algorithm can be visualized in the **Figures** commencing from **9** to **22**. Moreover, Tumor region and edema portion disintegration is also done using the proposed algorithm, which cannot be delivered by other competitive algorithms. It is conclusive that all the algorithms utilized for comparison in this paper have both advantages and disadvantages equally, with an exception for the proposed algorithm, which offers entrusting segmentation results.

Table 2 defines the efficacy of the proposed SOM – FKM algorithm using SI, OF, EF and Sensitivity values. The proposed technique outperforms FCM, SOM, FKM and other hybrid algorithms by providing better SI, OF and specificity values. EF value is sizably reduced using SOM based FKM algorithm. For a good image segmentation algorithm, SI and OF value should be close to 1 and EF value should be very nearer to 0 **[11]**. Afore mentioned values listed in **table 2** make a confirmation that the proposed hybrid SOM – FKM algorithm is superior to other image segmentation algorithms.

Fig. 29 has been completely derived from the comparison of sensitivity values produced by the proposed algorithm and other algorithms suggested by Khayati et al **[11]**, Johnston et al **[50]**, Boudraa et al **[51]**, Leemput et al **[52]**, Zijdenbos et al **[53]** and Hassan Khotanlou et al **[54]**. The proposed SOM based FKM algorithm is far superior to other rival segmentation techniques as it is produces 0.8718 as sensitivity.

7. Conclusion:

A novel hybrid SOM based FKM algorithm has been proposed through this paper and the recommended hybrid SOM – FKM algorithm excels FCM algorithm in the process of segmenting MR brain images. The effectiveness of the proposed algorithm is demonstrated

using **Tables 1, 2 & Fig.29**. Varied clinical datasets along with standard database images have been used to prove the efficacy of the proposed algorithm. A novel automated technique which requires minimal manual intervention to segment the tissues of brain, especially GM, WM and CSF regions, along with the identification of different types of tumor at different locations has been proposed through this paper. Moreover, MR brain image sequences of all three planes have been used in this research. The ultimate goal of this research work is to assist the clinician or radio surgeon in diagnosing the patients within reduced time duration and is greatly achieved through the combination of SOM and FKM techniques. Future work lies with improving the values of DOI, TC and PSNR values. Time duration for processing the images and MSE values can also be further reduced. The proposed algorithm can be extensively used in pre and post radio surgical applications.

Conflict of Interest:

The author(s) confirm that this article content has no conflicts of interest.

Acknowledgments:

The authors thank Dr. K.G. Srinivasan, MD, RD, Consultant Radiologist and Dr. K.P. Usha Nandhini, DNB, KGS Advanced MR & CT Scan - Madurai, Tamilnadu, India, for supporting the research with the patient information and MR brain images. Also, the authors thank the Department of Instrumentation and Control Engineering of Kalasalingam University, (Kalasalingam Academy of Research and Education), Tamilnadu, India for permitting to use the computational facilities available in biomedical laboratory which was set up with the support of the Department of Science and Technology (DST), New Delhi under FIST program.

References:

[1] Dr.N.Nandha Gopal: Automatic Detection of Brain Tumor through Magnetic Resonance Image. International Journal of Advanced Research in Computer and Communication Engineering, Vol: 2, Issue 4, April 2013.

[2] Govindaraj Vishnuvarthanan and Murugan Pallikonda Rajasekeran: Segmentation of MR Brain Images for Tumor Extraction Using Fuzzy, International Journal on Current Medical Imaging and Reviews CMIR, 9(1), 2013.

[3] El-Hachemi Guerrout, Ramdane Mahiou and Samy Ait-Aoudia: Medical Image Segmentation on a Cluster of PCs using Markov Random Fields. International Journal of New Computer Architectures and their Applications (IJNCAA), The Society of Digital Information and Wireless Communications (SDIWC) 3(1): 35-44 (ISSN: 2220-9085), 2013.

[4] E. Ben George and M.Karnan: MR Brain Image Segmentation using Bacteria Foraging Optimization Algorithm. International Journal of Engineering and Technology, Vol:4, No:5, Oct - Nov 2012.

[5] Sultan Aljahdali and E. A. Zanaty: Automatic Fuzzy Algorithms for Reliable Image Segmentation. IJCA, Vol. 19, No. 3, Sept. 2012.

[6] Sultan Aljahdali and E. A. Zanaty: Improving Fuzzy Algorithms for Automatic Image Segmentation. IEEE, 978-1-61284-732-0/11, 2010.

[7] K.Somasundaram and T. Kalaiselvi: Fully automatic brain extraction algorithm for axial T2-weighted magnetic resonance images. Computers in Biology and Medicine 40 (2010) 811–822.

[8] P.Vasuda and S.Satheesh: Improved Fuzzy C-Means Algorithm for MR Brain Image Segmentation, (IJCSE) International Journal on Computer Science and Engineering Vol. 02, No. 05, 1713-1715, 2010.

[9] T. Logeswari and M. Karnan: An improved implementation of brain tumor detection using segmentation based on soft computing. Journal of Cancer Research and Experimental Oncology Vol. 2(1). 006-014, March - 2010.

[10] T.Logeswari and M.Karnan: An Improved Implementation of Brain Tumor Detection Using Segmentation Based on Hierarchical Self Organizing Map. International Journal of Computer Theory and Engineering, Vol. 2, No. 4, 1793 - 8201 - 591, August 2010.

[11] Rasoul Khayati, Mansur Vafadusta, Farzad Towhidkhaha and S. Massood Nabavi: Fully automatic segmentation of multiple sclerosis lesions in brain MRFLAIR images using adaptive mixtures method and Markov random field model. Computers in Biology and Medicine, 38 (2008) 379 – 390,.

[12] Artem Mikheev, Gregory Nevsky, Siddharth Govindan, Robert Grossman and Henry Rusinek: Fully Automatic Segmentation of the Brain from T1-Weighted MRI Using Bridge Burner Algorithm. Journal of Magnetic Resonance Imaging, 27: (2008) 1235–1241.

[13] Yan Li and Zheru Chi: MR Brain Image Segmentation Based on Self-Organizing Map Network. International Journal of Information Technology Vol. 11, No. 8, 2005.

[14] Kohonen, Teuvo: Self-Organized Formation of Topologically Correct Feature Maps. Biological Cybernetics 43 (1): 1982, 59–69.

[15] Chih-Tang Chang et al: A Fuzzy K-Means Clustering Algorithm Using Cluster Center Displacement. Journal of information science and engineering, 27 (2011) 995-1009.

[16] Andac Hamamci, Nadir Kucuk, Kutlay Karaman, Kayihan Engin and Gozde Unal, Tumor-Cut: Segmentation of Brain Tumors on Contrast Enhanced MR Images for Radiosurgery Applications, IEEE transactions on medical imaging, vol. 31, 2011, 3.

[17] Meritxell Bach Cuadra, Claudio Pollo, Anton Bardera, Olivier Cuisenaire, Jean-Guy Villemure and Jean-Philippe Thiran, Atlas-Based Segmentation of Pathological MR Brain Images Using a Model of Lesion Growth, IEEE transactions on medical imaging, vol. 23, no. 10, October 2004.

[18] Karan Sikka, Nitesh Sinha, Pankaj K. Singh, Amit K. Mishra, A fully automated algorithm under modified FCM framework for improved brain MR image segmentation, Magnetic Resonance Imaging 27 (2009) 994–1004.

[19] A. Ortiz, J.M. Gorriz, J. Ramírezb, D. Salas-Gonzalez and J.M. Llamas-Elvira, Two fully-unsupervised methods for MR brain image segmentation using SOM-based strategies, Applied soft computing, 13 (2013) 2668–2682.

[20] Welstead and Stephen T Fractal, wavelet image compression techniques, SPIE Publication, ISBN 978-0-8194-3503-3, 155–156.

[21] Thomos N, Boulgouris N. V and Strintzis, M. G, Optimized Transmission of JPEG2000 Streams Over Wireless Channels, IEEE Transactions on Image Processing, 2006, 15 (1).

[22] Vida Harati, Rasoul Khayati and Abdolreza Farzan, Fully automated tumor segmentation based on improved fuzzy connectedness algorithm in brain MR images, Computers in Biology and Medicine, 41(2011) 483–492.

[23] Yu J and Yang M.S, Optimality test for generalized FCM and its application to parameter selection, IEEE Trans. Fuzzy Syst. 13 (2), 2005, 164–176.

[24] Yu J and Yang M.S, A generalized fuzzy clustering regularization model with optimality tests and model complexity analysis, IEEE Trans. Fuzzy Syst. 15 (5), 2007, 904–915.

[25] Shen S, Sandham W, Granat M and Sterr A, MRI fuzzy segmentation of brain tissue using neighborhood attraction with neural-network optimization, IEEE Trans. Inf. Technol. Biomed. 9, 2005, 459–467.

[26] A. Riad, A. Atwan, H. El-Bakry, R. Mostafa, H. Elminir and N. Mastorakis, A new approach for segmentation of MR brain image, in: Proceedings of the WSEAS International Conference on Environment, Medicine and Health Sciences, 2010.

[27] T. Kapur, W. Grimson, I. Wells and R. Kikinis, Segmentation of brain tissue from magnetic resonance images, Medical Image Analysis 1 (2) (1996) 109–127.

[28] Y. Tsai, I. Chiang, Y. Lee, C. Liao, K. Wang, Automatic MRI meningioma segmentation using estimation maximization, in: Proceedings of the 27th IEEE Engineering in Medicine and Biology Annual Conference, 2005.

[29] J. Xie, H. Tsui, Image segmentation based on maximum-likelihood estimation and optimum entropy distribution (MLE-OED), Pattern Recognition Letters 25 (2005) 1133–1141.

[30] S. Smith, M. Brady, Y. Zhang, Segmentation of brain images through a hidden Markov random field model and the expectation-maximization algorithm, IEEE Transactions on Medical Imaging 20 (1) (2001).

[31] W. Wells, W. Grimson, R. Kikinis, F. Jolesz, Adaptive segmentation of MRI data, IEEE Transactions on Medical Imaging 15 (4) (1996) 429–442.

[32] N. Mohamed, M. Ahmed, A. Farag, Modified fuzzy c-mean in medical image segmentation, in: IEEE International Conference on Acoustics, Speech and Signal Processing, 1999.

[33] G. Liyuan, C. Wanhua, X. Haixiang, Performance evaluation of SVM in image segmentation, in: Proceedings of the ICSP 2008 International Conference, 2008.

[34] V. Vapnik, Statistical Learning Theory, Wiley, New York, 1998.

[35] C. Parra, K. Iftekharuddin, R. Kozma, Automated brain tumor segmentation and pattern recognition using AAN, in: Proceedings of the 2nd International Conference on Computational Intelligence, Robotics and Autonomous Systems, December 2003.

[36] P. Sahoo, S. Soltani, A. Wong, Y. Chen, A survey of thresholding techniques, Computer Vision, Graphics, and Image Processing 41 (2) (2010) 233–260.

[37] Z. Yang, J. Laaksonen, Interactive Retrieval in Facial Image Database Using Self-Organizing Maps, MVA, 2005.

[38] I. Guler, A. Demirhan, R. Karakis, Interpretation of MR images using self-organizing maps and knowledge-based expert systems, Digital Signal Processing 19 (2009) 668–677.

[39] S. Ong, N. Yeo, K. Lee, Y. Venkatesh, D. Cao, Segmentation of color images using a two-stage self-organizing network, Image and Vision Computing 20 (2002) 279–289.

[40] J. Alirezaie, M. Jernigan, C. Nahmias, Automatic segmentation of cerebral MR images using artificial neural networks, IEEE Transactions on Nuclear Science 45 (4) (1998) 2174–2182.

[41] W. Sun, Segmentation method of MRI using fuzzy Gaussian basis neural network, Neural Information Processing 8 (2) (2005) 19–24.

[42] L. Fan, D. Tian, A brain MR images segmentation method based on SOM neural network, in: IEEE International Conference on Bioinformatics and Biomedical Engineering, 2007.

[43] Y. Jiang, K. Chen, Z. Zhou, SOM based image segmentation, in: Proceedings of the 9th International Conference on Rough Sets, Fuzzy Sets, Data Mining, and Granular Computing, 2003.

[44] E. Alhoniemi, J. Himberg, J. Parhankagas and J. Vesanta, SOM Toolbox for Matlab v2.0, <http://www.cis.hut.fi/projects/somtoolbox>, 2005.

[45] D. Salas-Gonzalez, M. Schlogl, J.M. Gorriz, J. Ramirez, E.W. Lang, Bayesian segmentation of magnetic resonance images using the α-stable distribution, in: International Conference on Hybrid Artificial Intelligence Systems, HAIS, 2011.

[46] E. Arsuaga, F. Díaz, Topology preservation in SOM, International Journal of Mathematical and Computer Sciences 1 (1) (2005) 19–22.

[47] T. Kohonen, Self-Organizing Maps, Springer, 2001.

[48] Brain Extraction tool (BET), FMRIB Centre, Nuffield Department of Neurosciences, University of Oxford, <http://www.fmrib.ox.ac.uk/analysis/research/bet/>.

[49] Govindaraj, V. and Murugan, P. R., A complete automated algorithm for segmentation of tissues and identification of tumor region in T1, T2, and FLAIR brain images using optimization and clustering techniques", Int. J. Imaging Syst. Technol, doi: 10.1002/ima.22108, 24 (2014) 313–325.

[50] B. Johnston, M.S. Atkins, B. Mackiewich and M. Anderson, Segmentation of multiple sclerosis lesions in intensity corrected multispectral MRI, IEEE Transactions on Medical Imaging 15 (1996) 154–169.

[51] A.O. Boudraa, S.M.R. Dehakb, Y.M. Zhu, C. Pachai, Y.G. Bao and J.Grimaud, Automated segmentation of multiple sclerosis lesions in multispectral MR imaging using fuzzy clustering, Computers in Biology and Medicines, 30(2000) 23–40.

[52] K.V. Leemput, F.Maes, D.Vandermeulen, A.Colchester and P.Suetens, Automated segmentation of multiple sclerosis lesions by model outlier detection, IEEE Transactions on Medical Imaging, 20 (2001) 677–688.

[53] A.P. Zijdenbos, R. Forghani, A.C. Evans, Automatic 'pipeline' analysis of 3-D MRI data for clinical trials: application to multiple sclerosis, IEEE Transactions on Medical Imaging, 20, (2001) 677–688, 21 (2002) 1280–1291.

[54] Hassan Khotanlou and Mahlagha Afrasiabi, Segmentation of Multiple Sclerosis Lesions in Brain MR Images using Spatially Constrained Possibilistic Fuzzy C-means Classification, Journal of Medical Signals & Sensors, Vol 1, issue 3, Sep-Dec 2011.

[55] Andres Ortiz, Antonio A. Palacio, Juan M. Gorriz, Javier Ramírez and Diego Salas-Gonzalez, Segmentation of Brain MRI Using SOM-FCM-Based Method and 3D Statistical Descriptors, Computational and Mathematical Methods in Medicine, Volume 2013 (2013), Article ID 638563, < http://dx.doi.org/10.1155/2013/638563> .

[56] A. Ortiz, J. M. Gorriz, J. Ramirez and D. Salas-Gonzalez, Unsupervised Neural Techniques Applied to MR Brain Image Segmentation, Advances in Artificial Neural Systems, Volume 2012 (2012), Article ID 457590, < http://dx.doi.org/10.1155/2012/457590>.

[57] J. Jiang, P. Trundle and J. Ren, Medical image analysis with artificial neural networks", Computerized Medical Imaging and Graphics 34 (2010) 617–631.

[58] K. Somasundaram and T.Kalaiselvi, Automatic brain extraction methods for T1 magnetic resonance images using region labelling and morphological operations, Computers in Biology and Medicine 41 (2011) 716–725.

[59] Jouko Lampinen and Timo Kostiainen, Self-Organizing Map in Data-Analysis - Notes on Over fitting and Over interpretation, Proc. ESANN'2000, Bruges, Belgium, 239-244.

[60] Rafael C. Gonzalez and Richard E. Woods, Digital Image Processing, Second Ed.., Pearson Education publication, ISBN 81 – 7808 – 629 – 8, pp.68 – 70.

[61] G.R. Sinha and Bhagawati Charan Patel, Medical Image Processing: Concepts and Applications, PHI publications, ISBN-978-81-203-4902-5, 2014.

Figures:

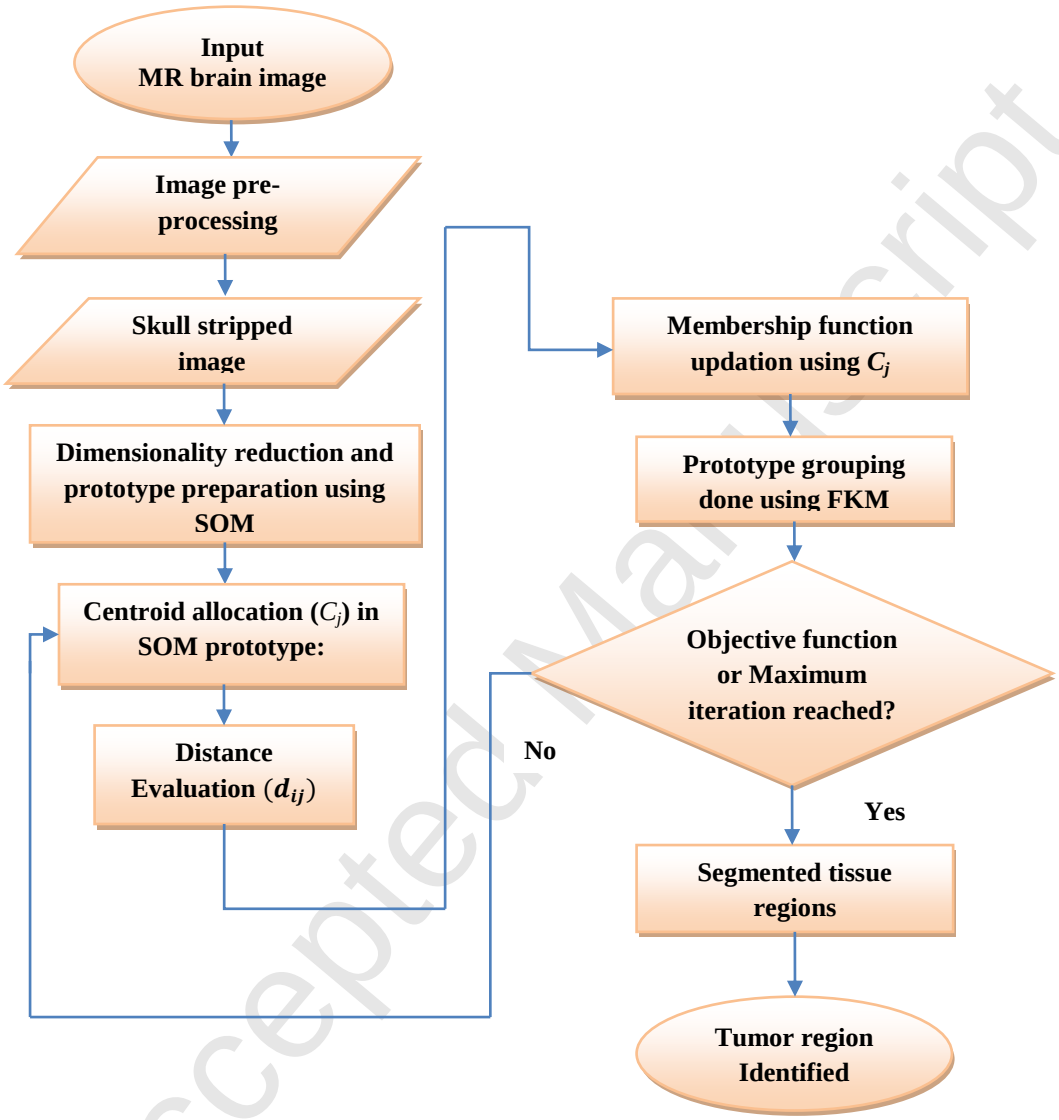

Fig. 1. Flowchart of hybrid SOM based FKM algorithm.

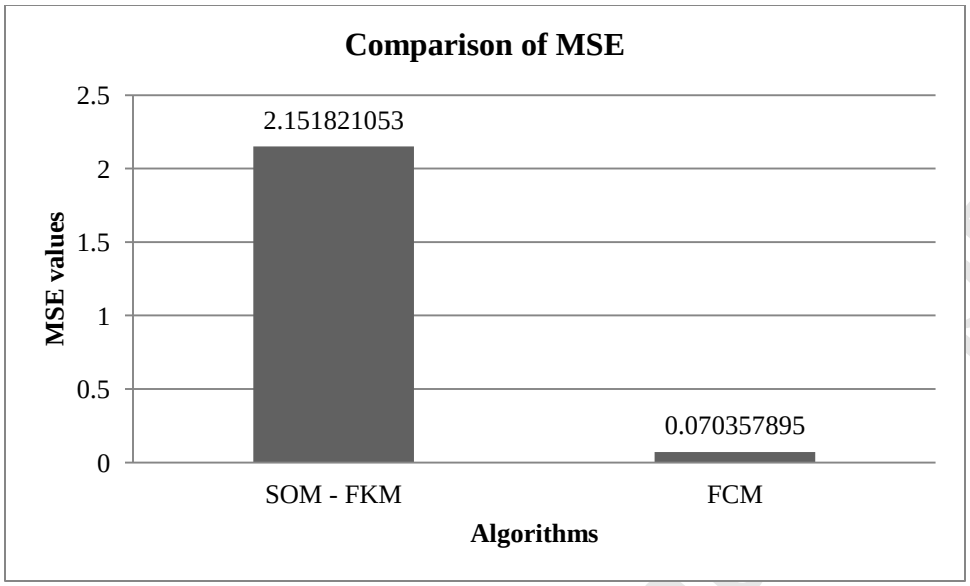

Fig. 2. Comparison of Mean Square Error values obtained from SOM – FKM and FCM algorithms.

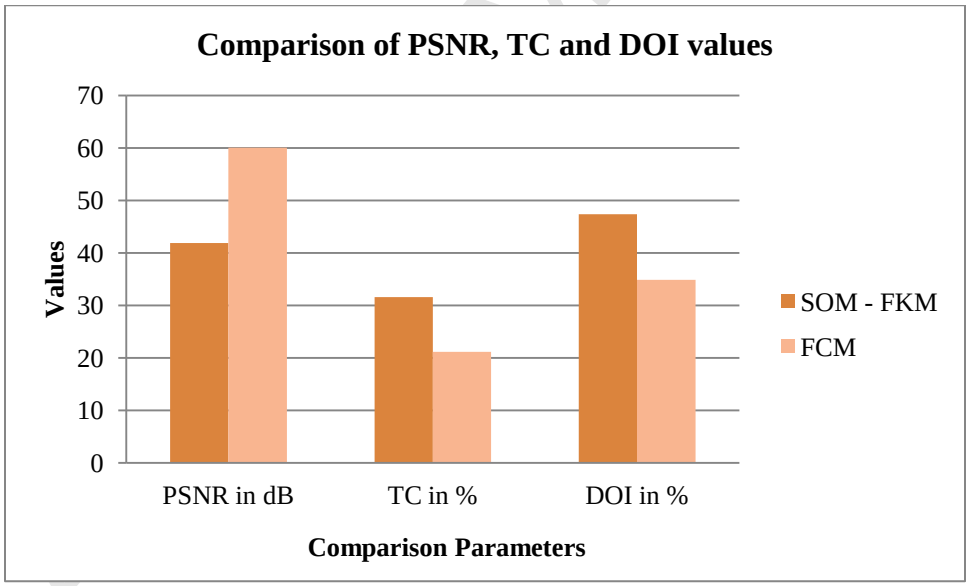

Fig. 3. Comparison of Peak Signal to Noise Ratio (PSNR), Tanimoto Coefficient (TC) and Dice Overlap Index (DOI) values obtained from SOM – FKM and FCM algorithms.

.

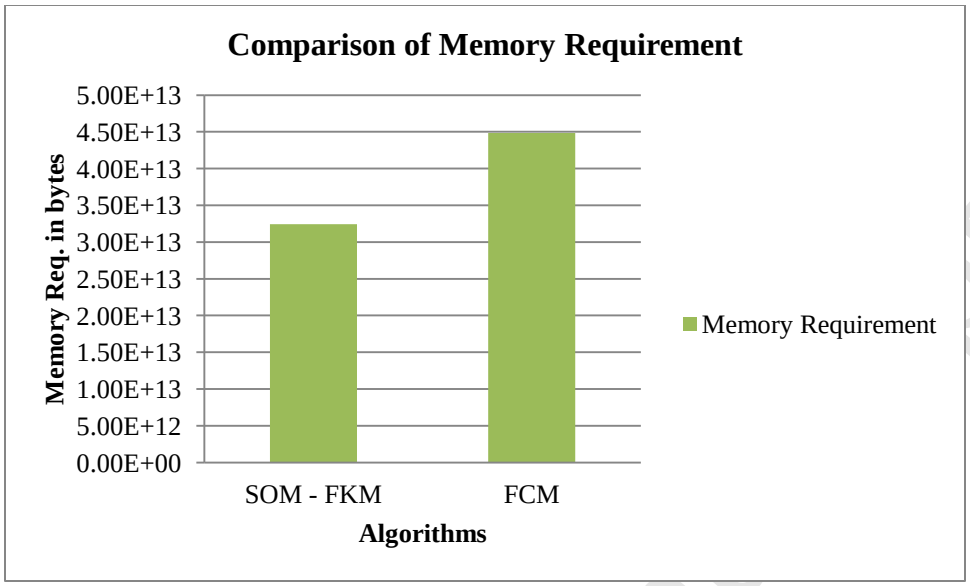

Fig. 4. Comparison of Memory Requirement or Memory Utilization values obtained from SOM – FKM and FCM algorithms.

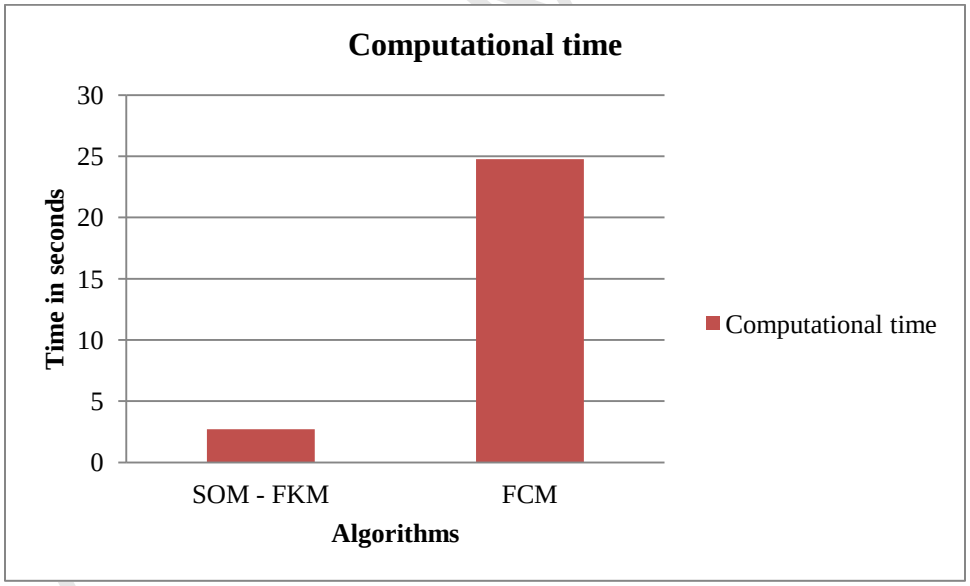

Fig. 5. Comparison of Computational Time or Elapsed Time values obtained from SOM – FKM and FCM algorithms.

Gold Standard Images of patient - 1 (age: 5)
suffering from Primitive Neuro Ectodermal tumor

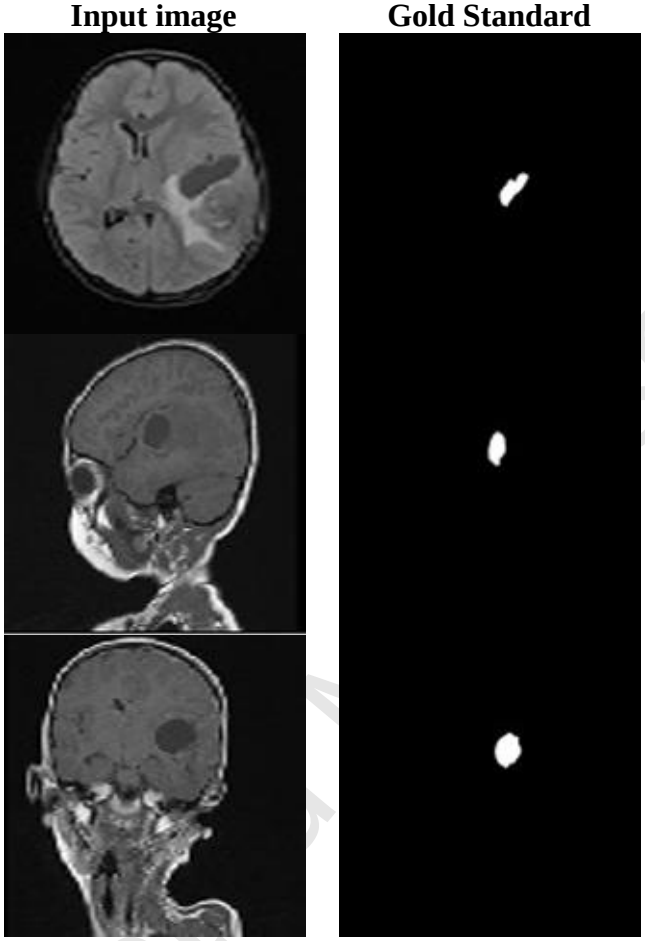

Fig. 6. Gold Standard Images of the tumor detected region for patient – 1.

Gold Standard Image for Harvard database

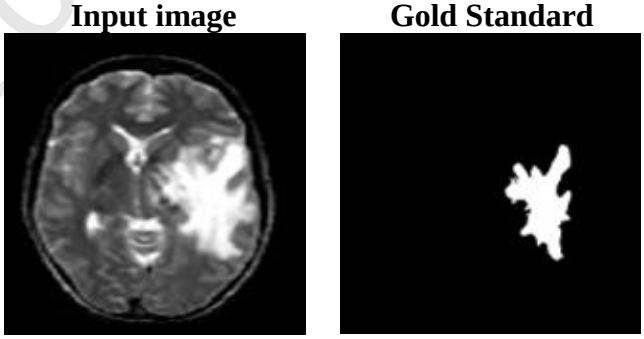

Fig. 7. Gold Standard Image of tumor detected region for the data available in Harvard Brain Web Repository.

Gold Standard Image for Harvard database

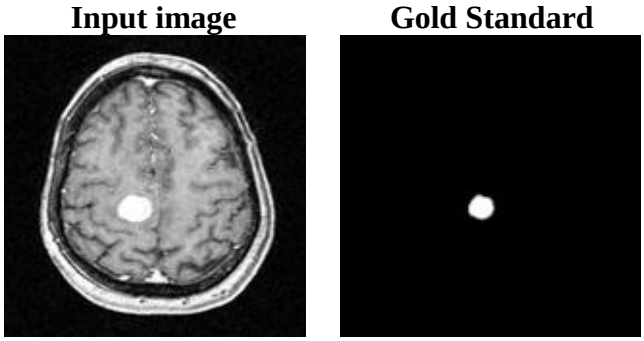

Fig. 8. Gold Standard Image of tumor detected region for the patient suffering from Nerve Sheath Tumors.

Segmentation Results from Hybrid SOM – FKM algorithm:

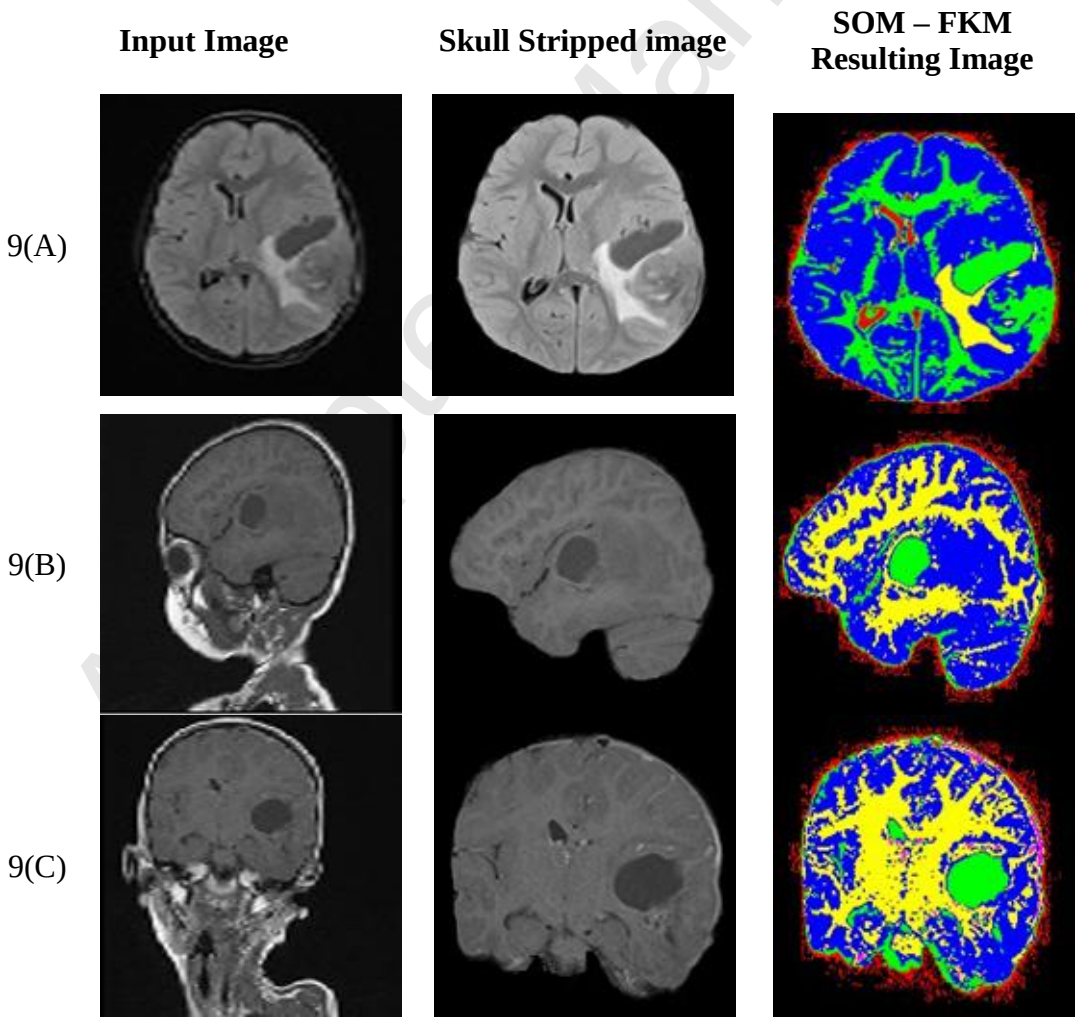

Fig. 9. Segmented results of patient - 1 (age: 5) suffering from Primitive Neuro Ectodermal tumor obtained from clinical database.

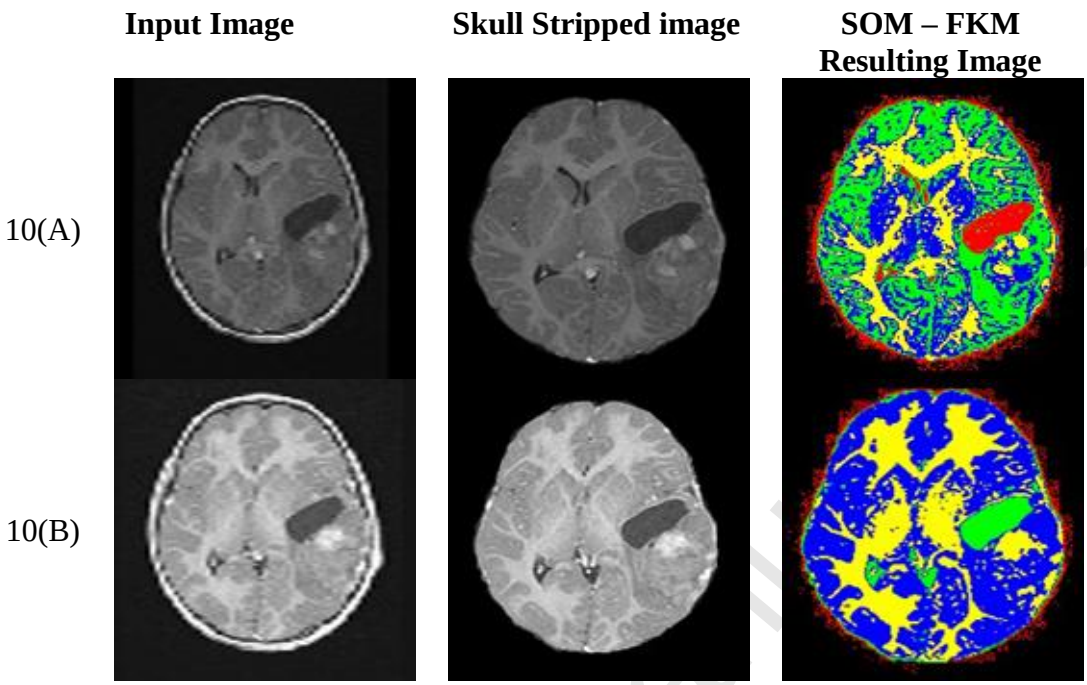

Fig. 10. Segmented results of patient - 1 (age: 5) suffering from Primitive Neuro Ectodermal tumor obtained from clinical database, which are of 3D Multi Planar Reconstruction (MPR) type images.

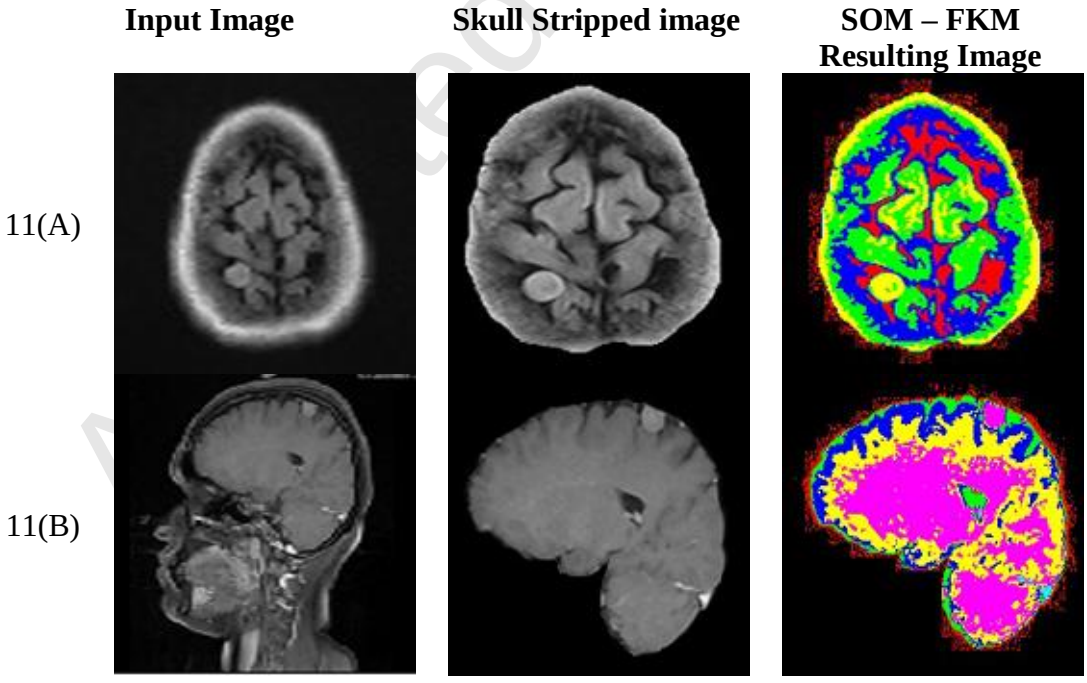

11(C)

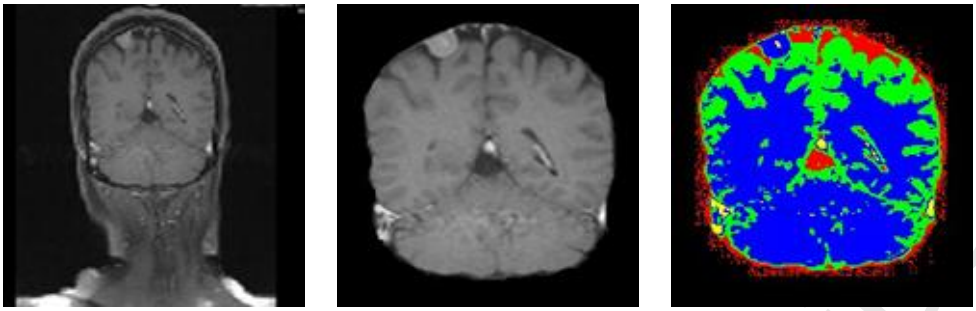

Fig. 11. Segmented results of patient - 2 (age: 35) suffering from Meningioma obtained from clinical database.

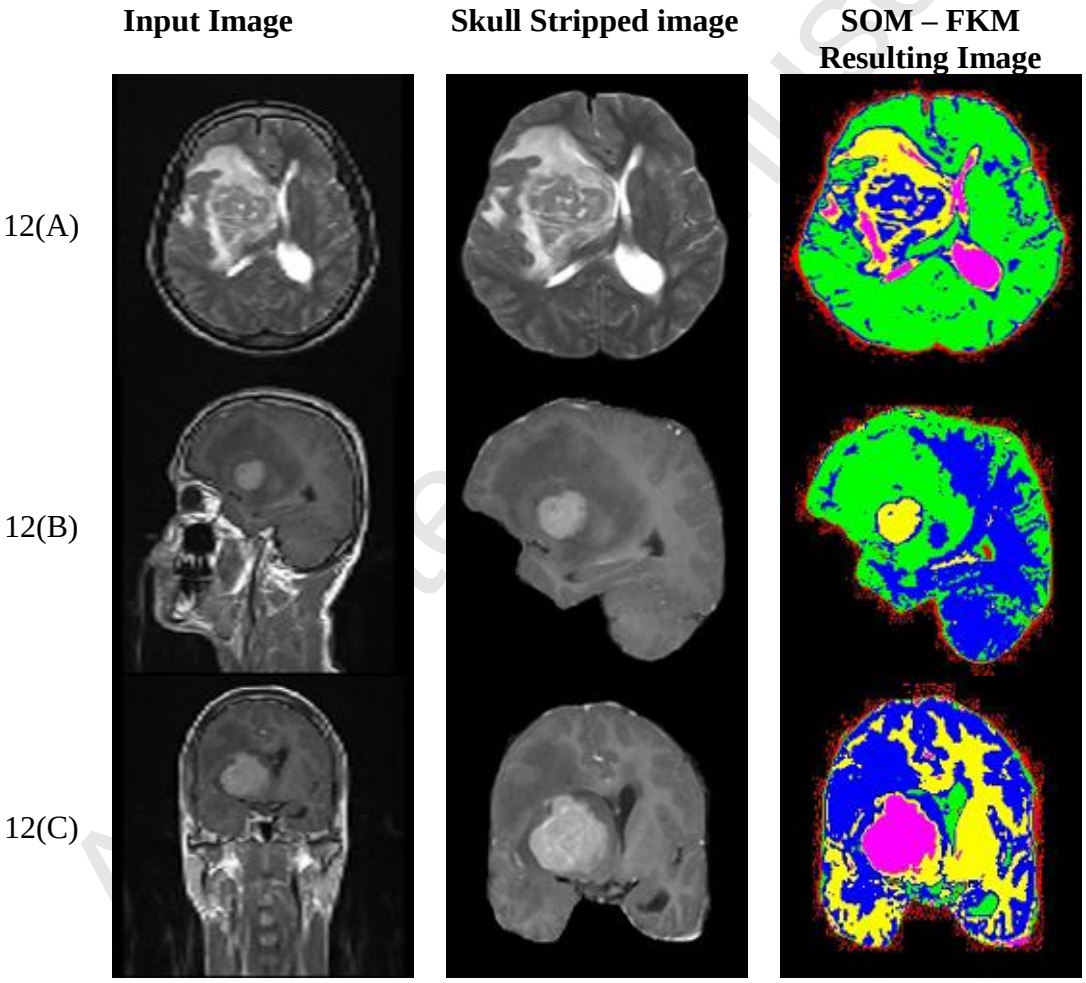

Fig. 12. Segmented results of patient - 3 (age: 32) suffering from high grade Astrocytoma obtained from clinical database.

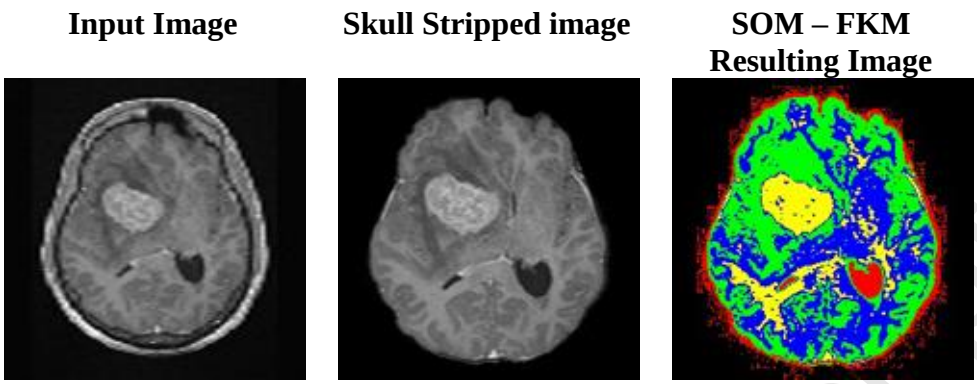

Fig. 13. Segmented result of patient - 3 (age: 32) suffering from high grade Astrocytoma obtained from clinical database, which is of 3D Multi Planar Reconstruction (MPR) type image.

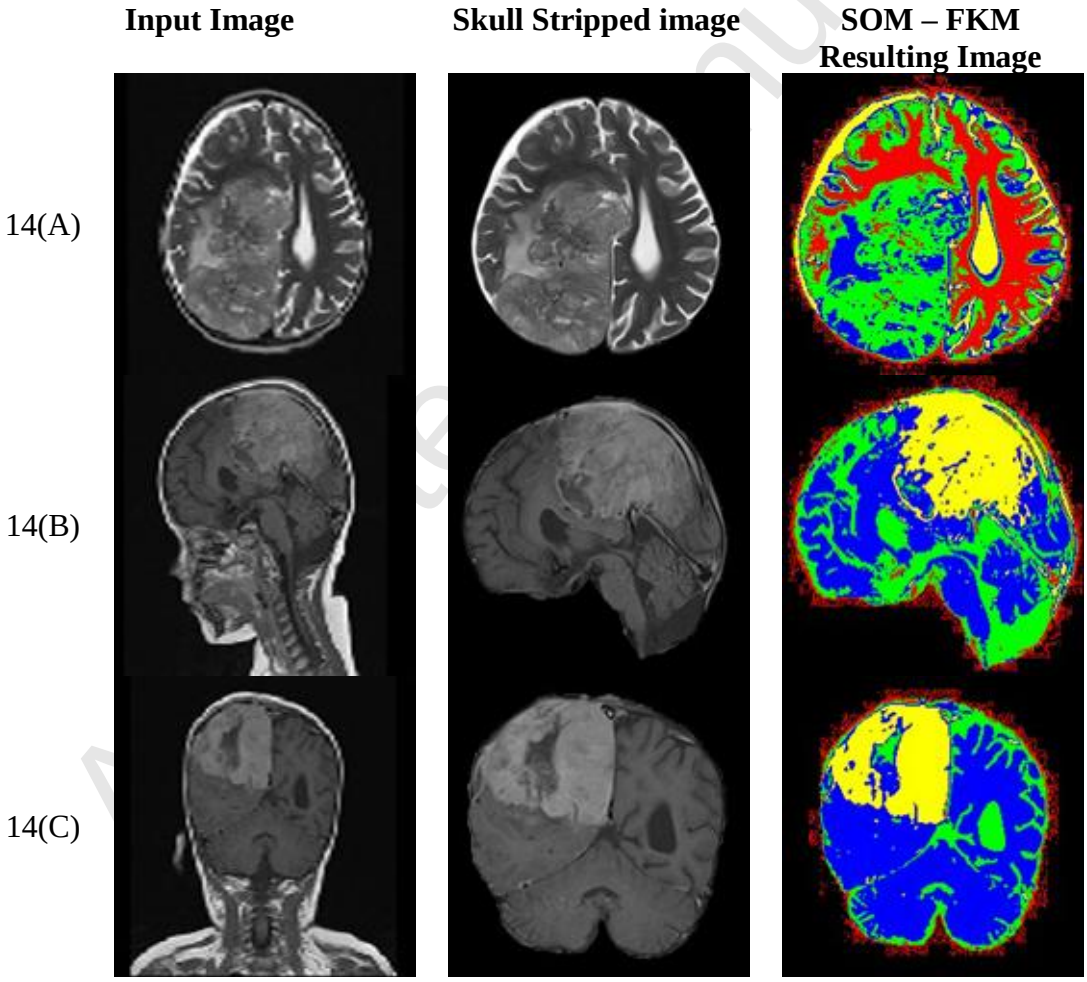

Fig. 14. Segmented results of patient - 4 (age: 3) suffering from supratentorial Primitive Neuro Ectodermal Tumor obtained from clinical database.

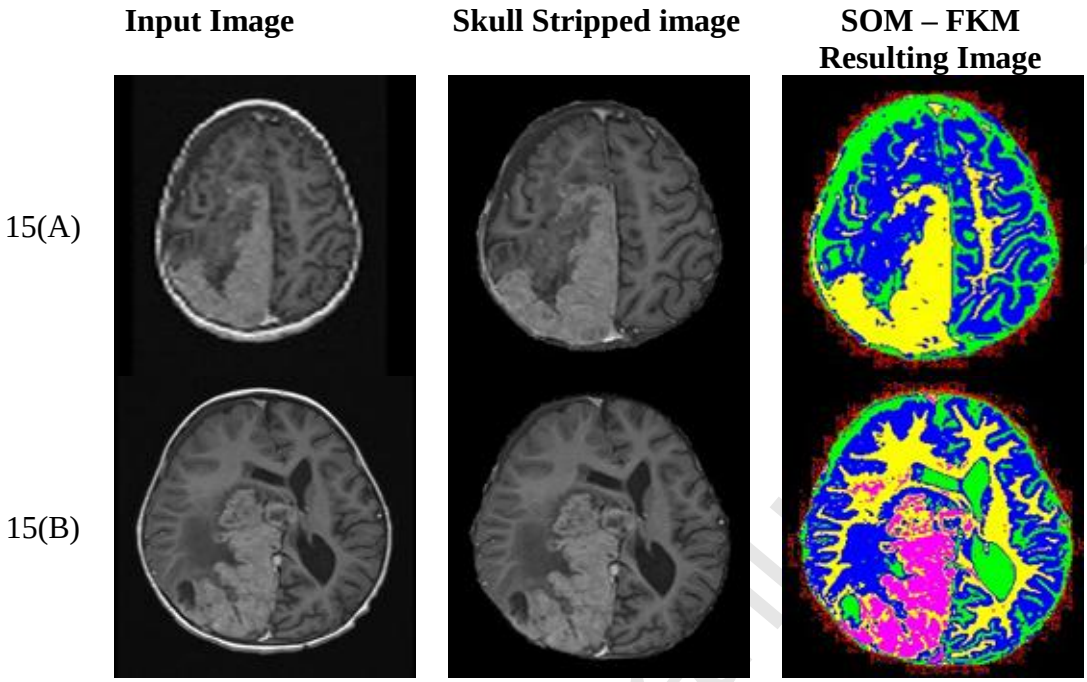

Fig. 15. Segmented results of patient - 4 (age: 3) suffering from supratentorial Primitive Neuro Ectodermal Tumor obtained from clinical database, which are of 3D Multi Planar Reconstruction (MPR) type images.

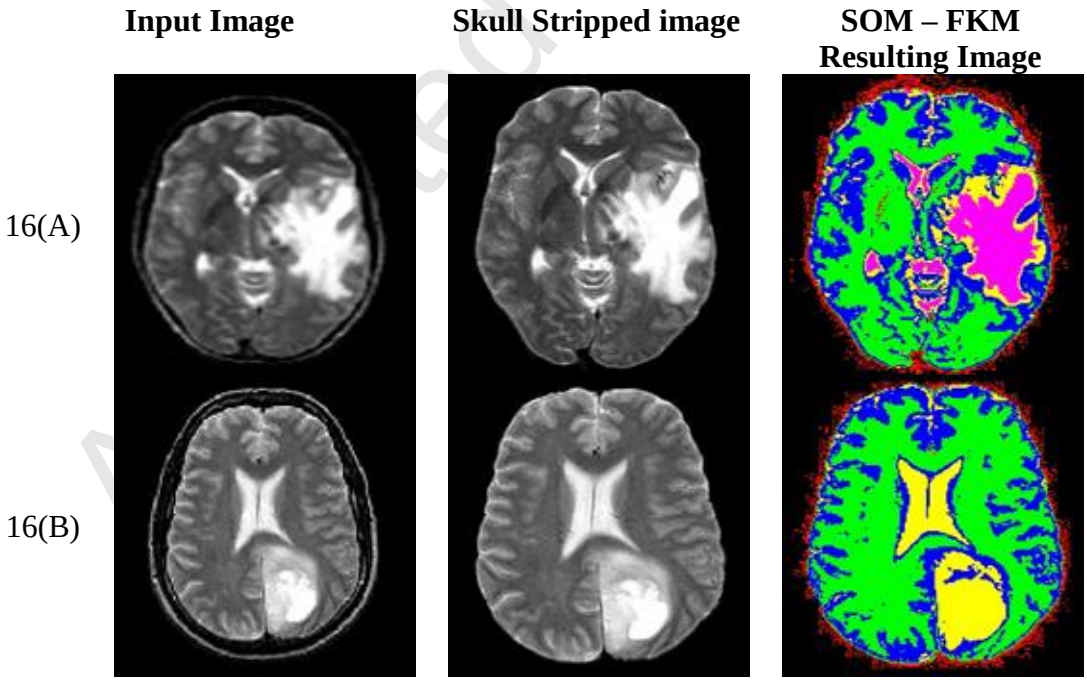

16(C)

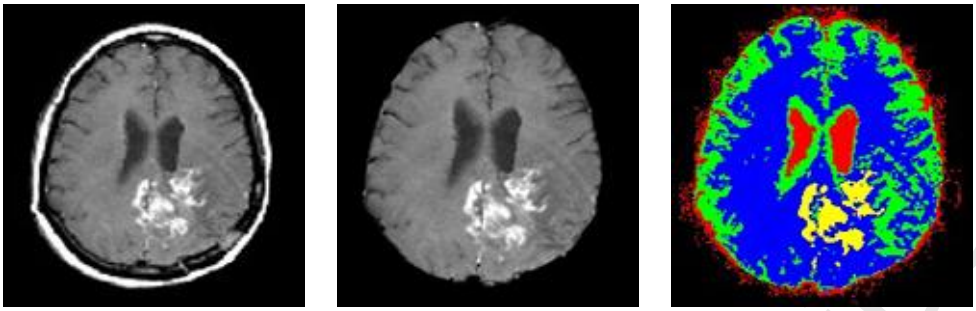

Fig. 16. Segmented results of the patients suffering from Glioma and Metastatic Bronchogenic Carcinoma, obtained from Harvard Brain Web Repository.

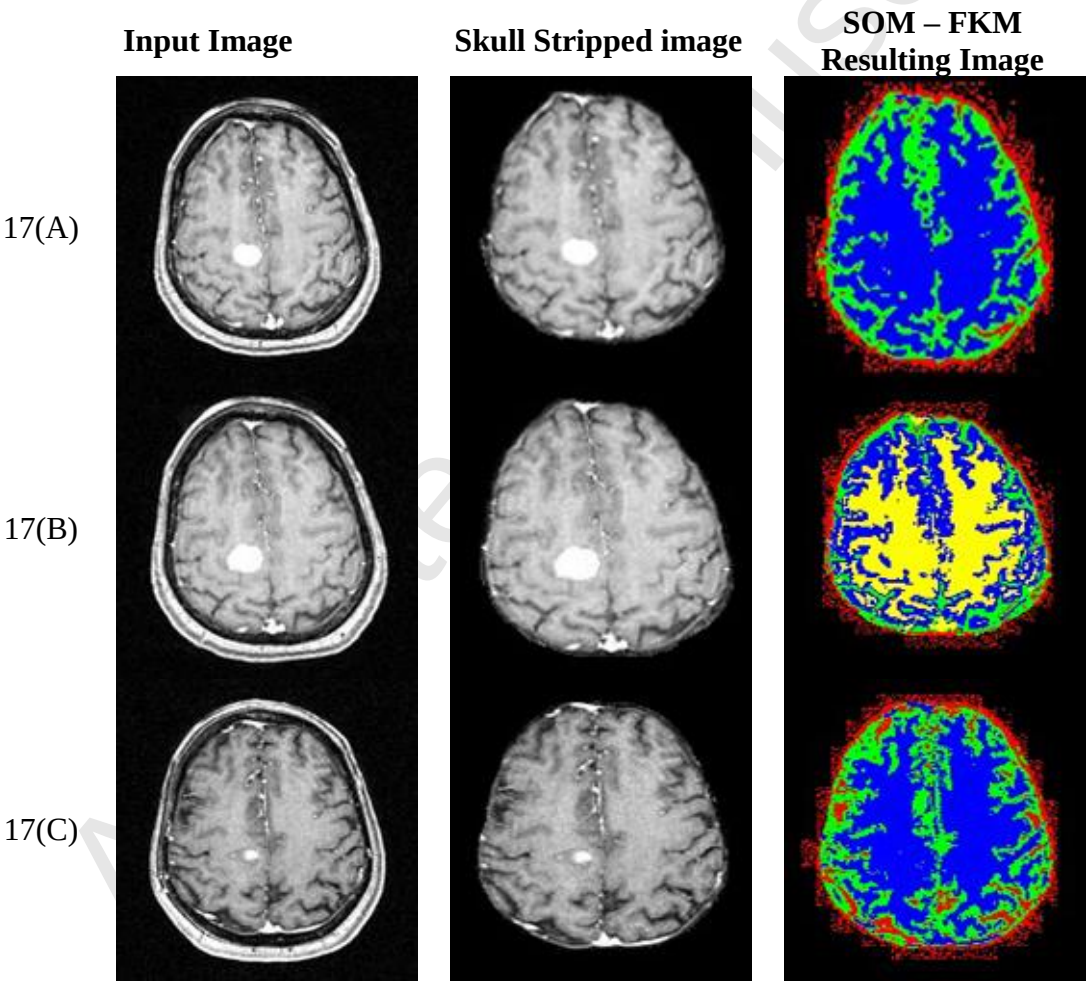

17 (D)

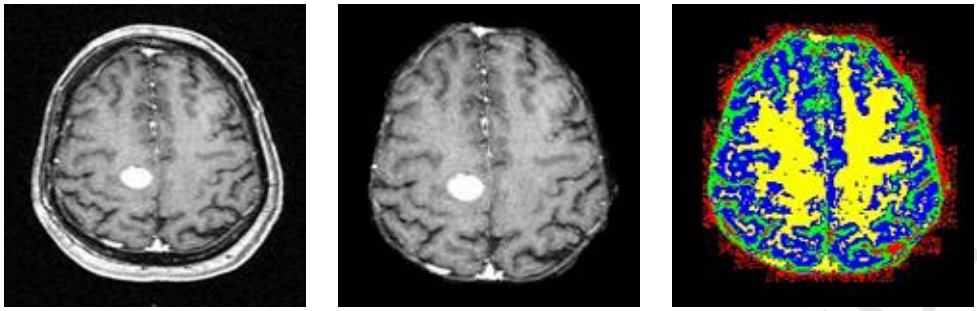

Fig. 17. Segmented results of the patients suffering from Pituitary Adenomas.

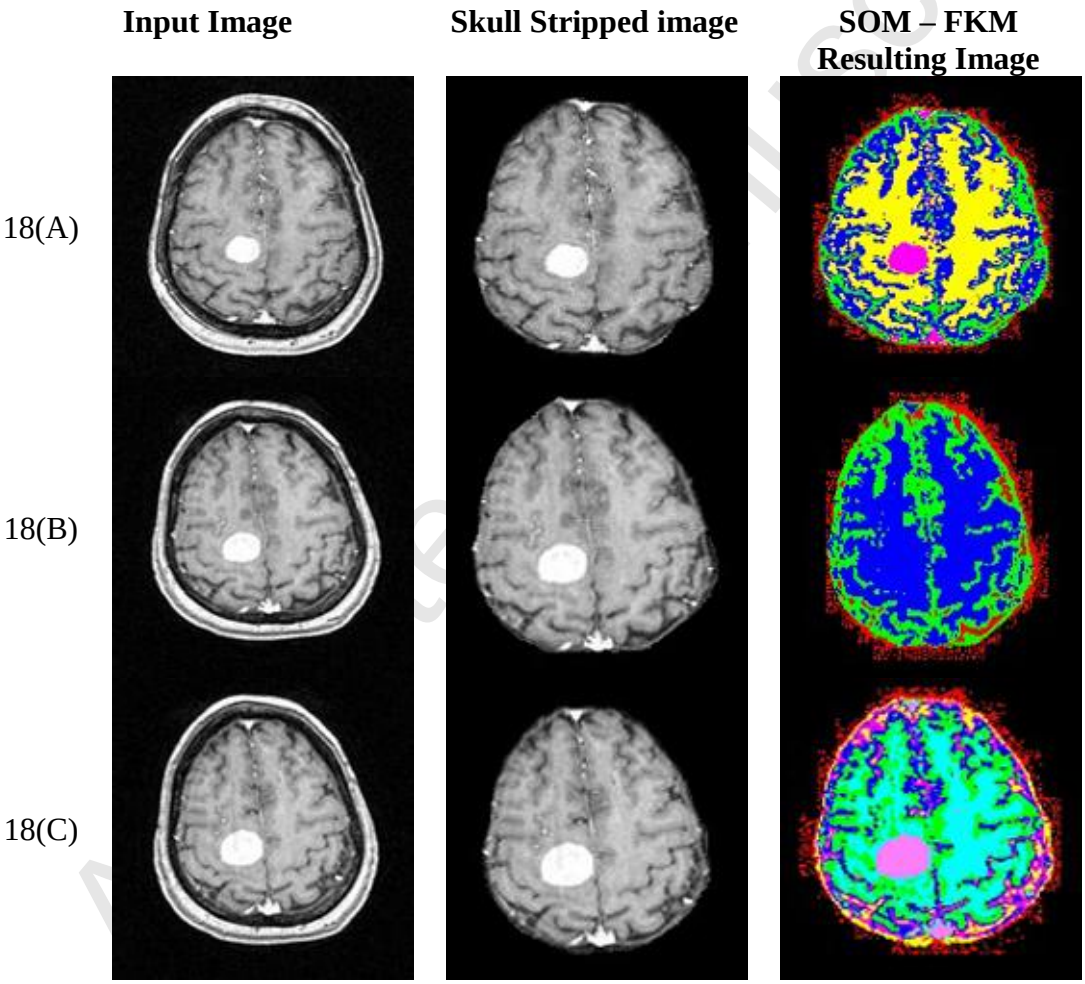

Fig. 18. Segmented results of the patients suffering from Nerve Sheath Tumors.

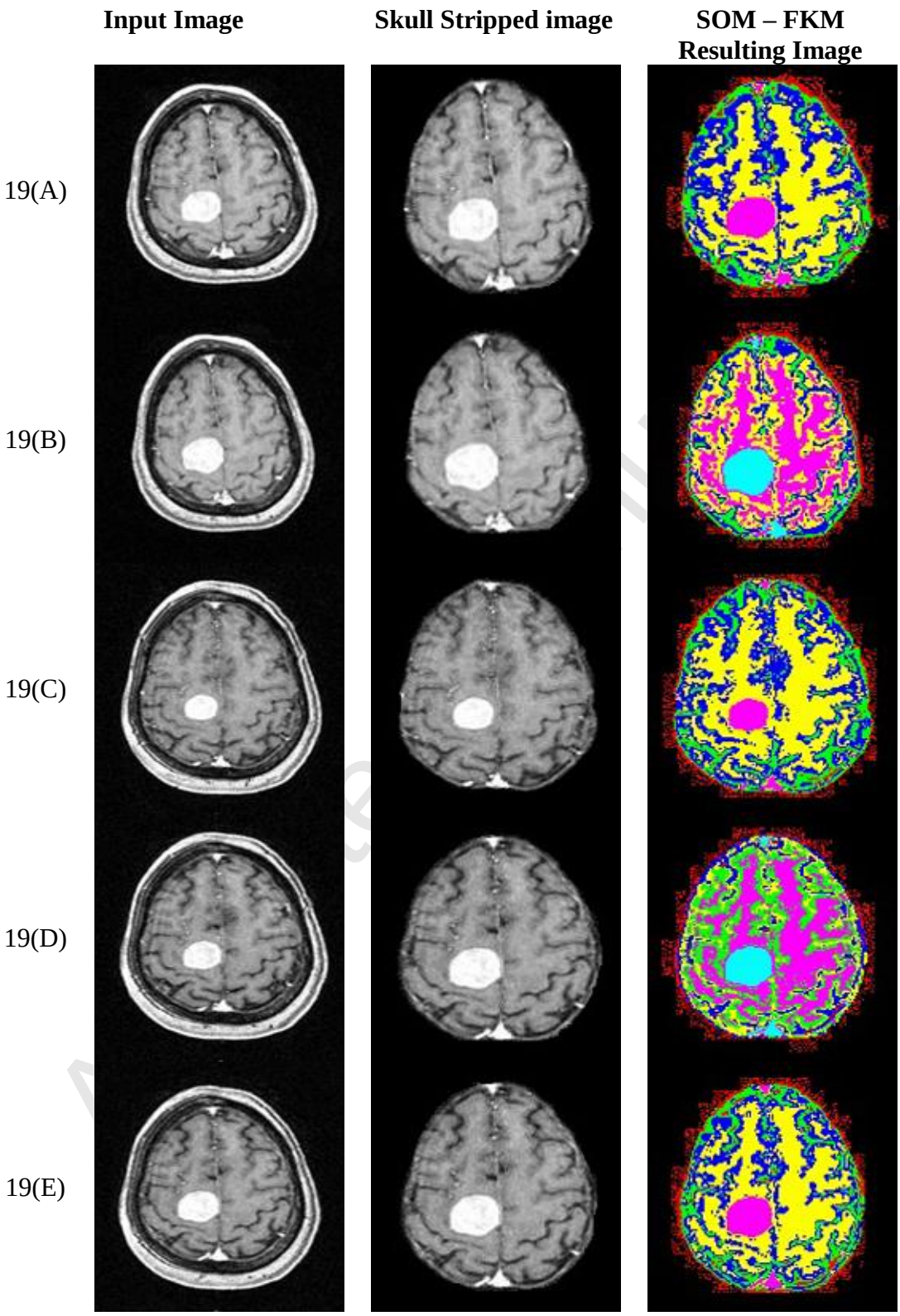

Fig. 19. Segmented results of the patients suffering from low grade Glioma.

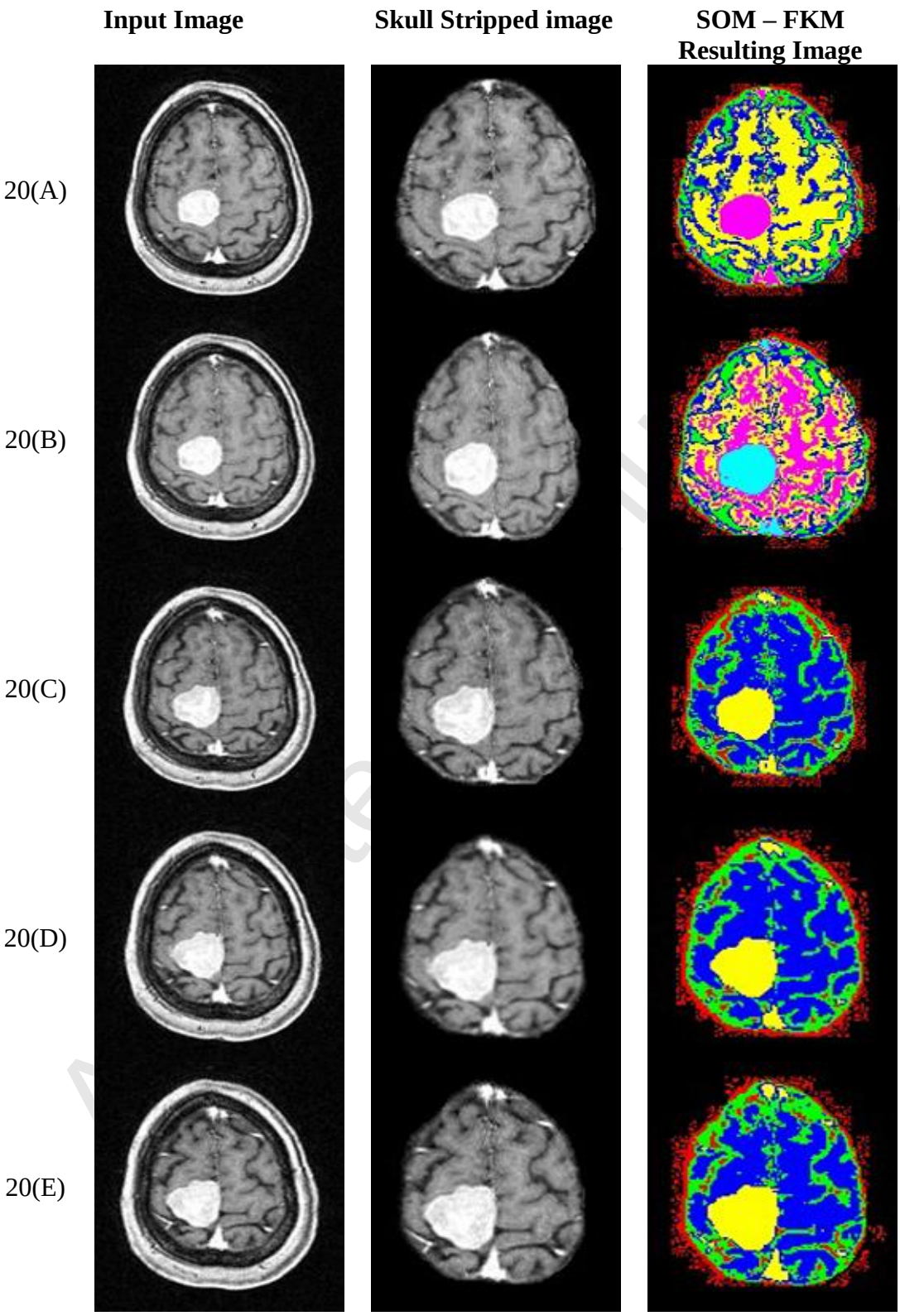

20(F)

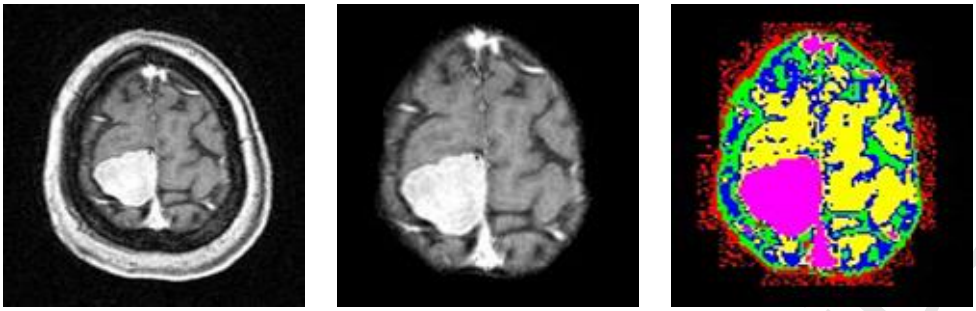

Fig. 20. Segmented results of the patients suffering from high grade Glioma.

21(A) 21(B) 21(C) 21(D)

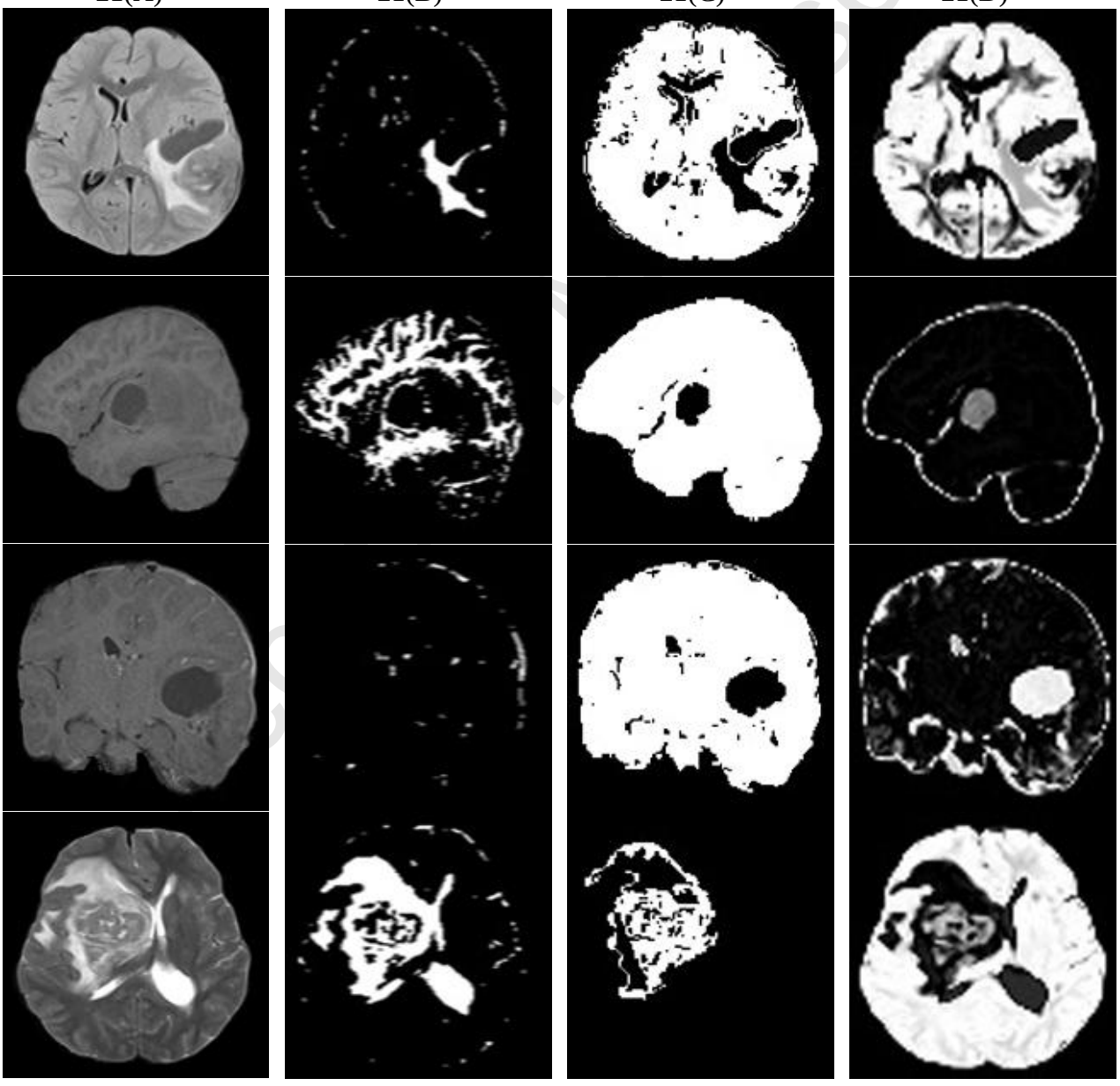

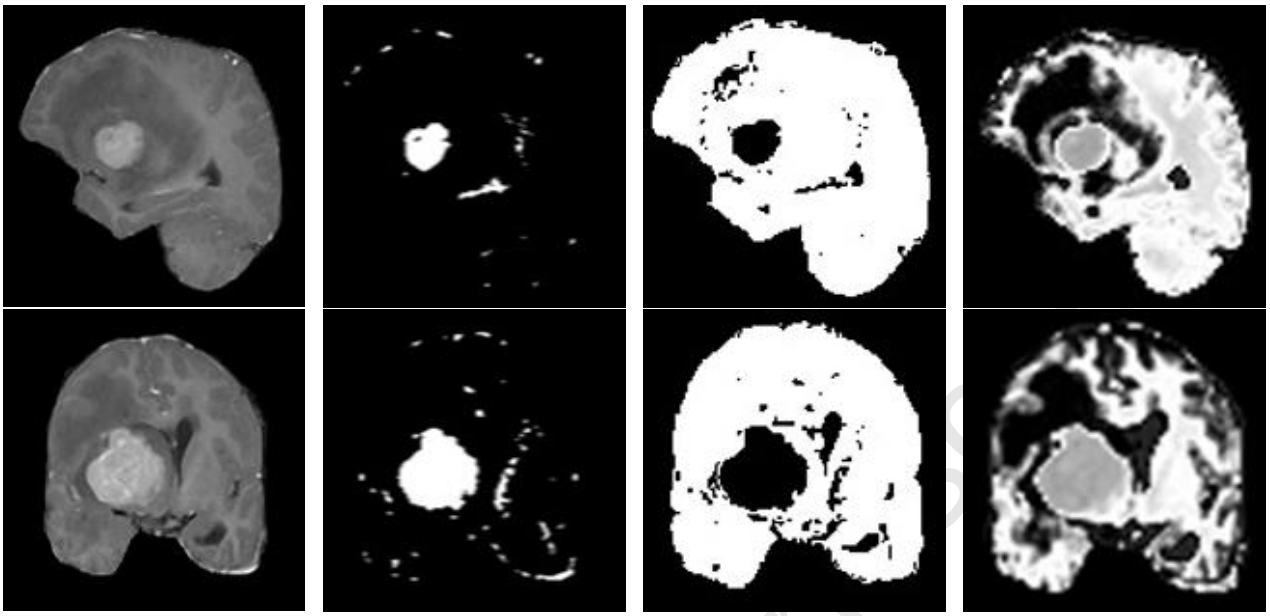

Fig. 21. Comparison of segmentation results derived from three different algorithms. **21(A)** Input images of patient – 1 & 3. Segmentation results obtained using **21(B)** Entropy based Fuzzy clustering, **21(C)** Graph based Fuzzy Clustering and **21(D)** kernel based Fuzzy Clustering.

22(A) 22(B) 22(C) 22(D)

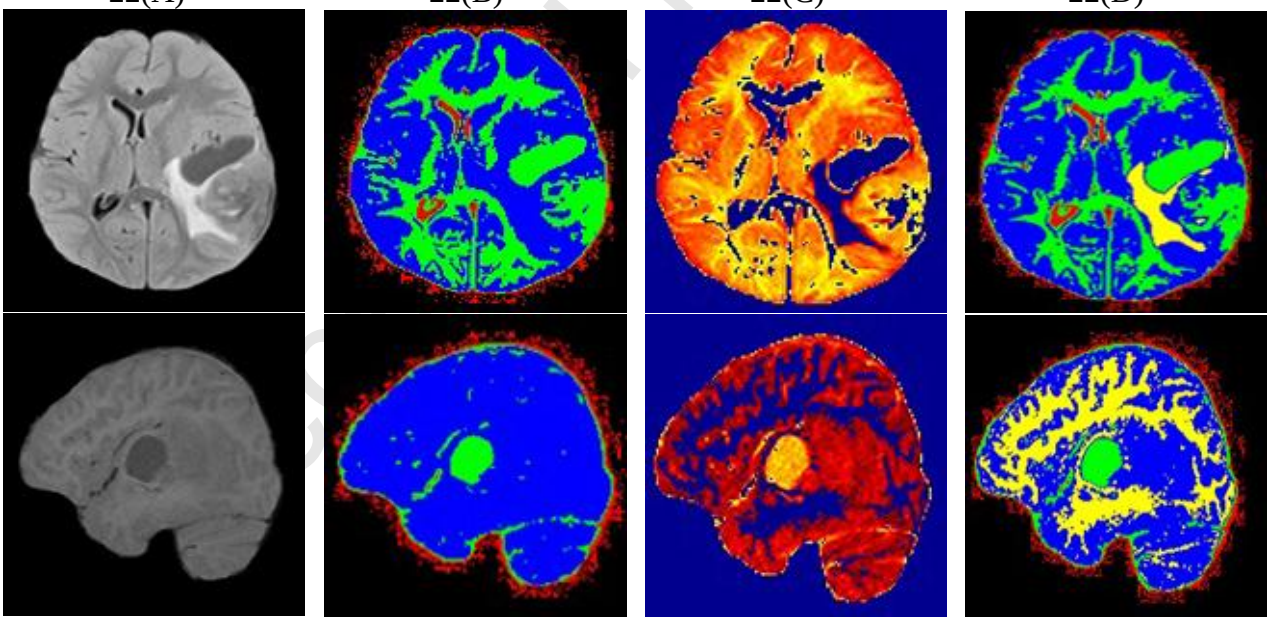

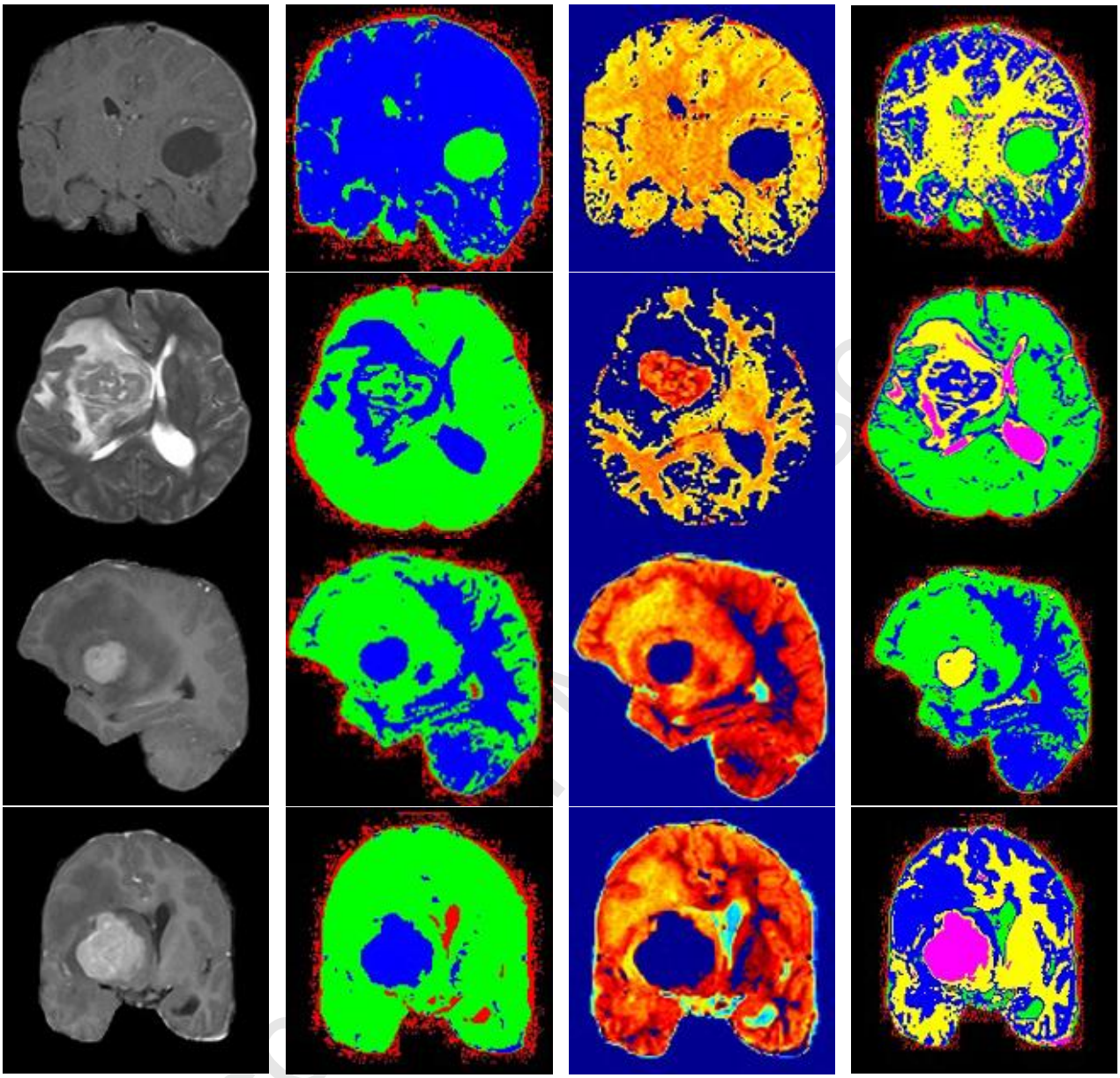

Fig. 22. Comparison of segmentation results derived from three algorithms extensively used in this work. **22(A)** Input images of patient – 1 & 3. Segmentation results obtained using **22(B)** SOM based clustering, **22(C)** FKM based Clustering and **22(D)** SOM – FKM based Clustering.

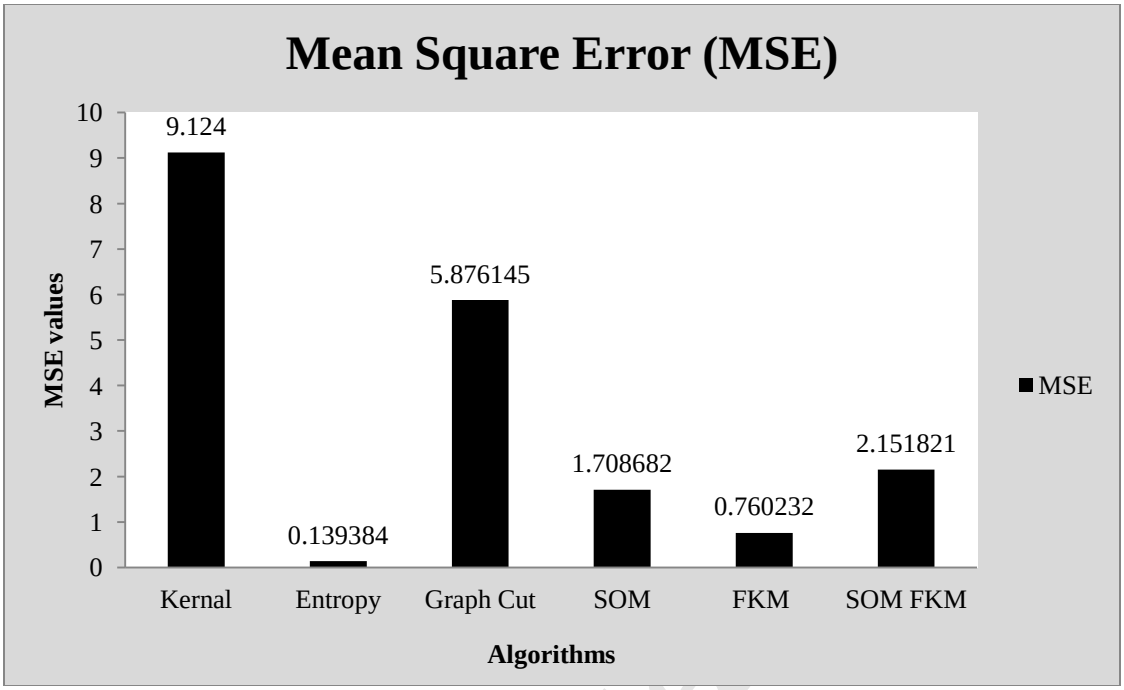

Fig. 23. Comparison of segmentation algorithms using MSE.

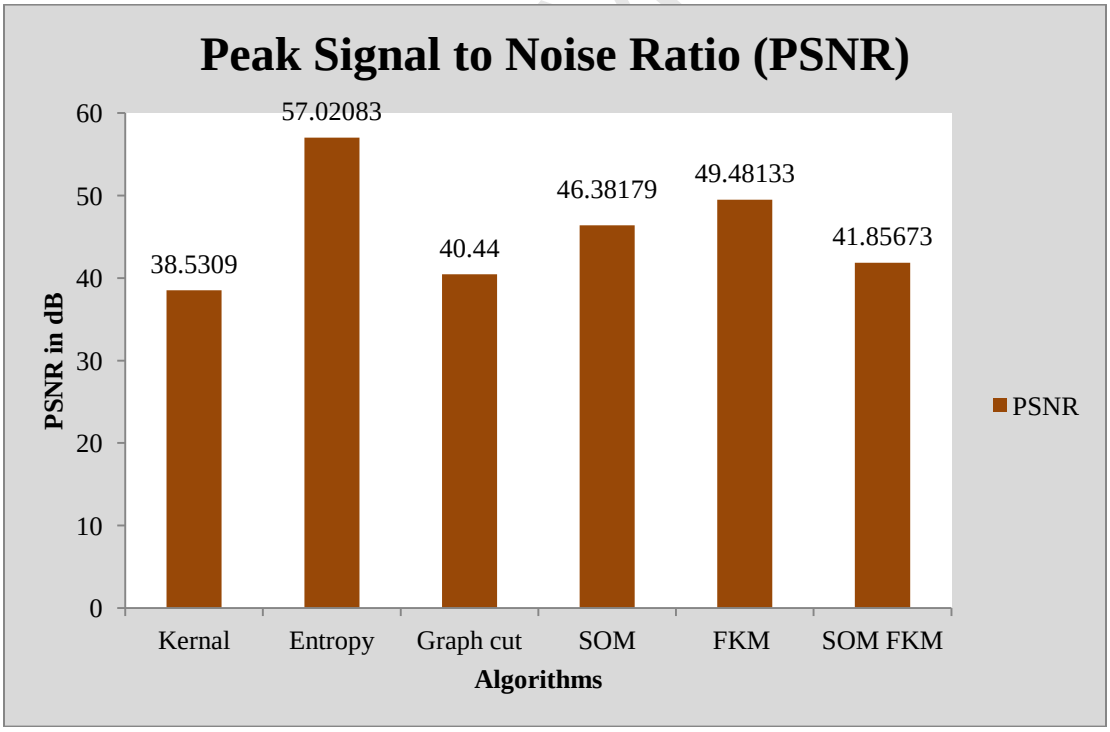

Fig. 24. Comparison of segmentation algorithms using PSNR.

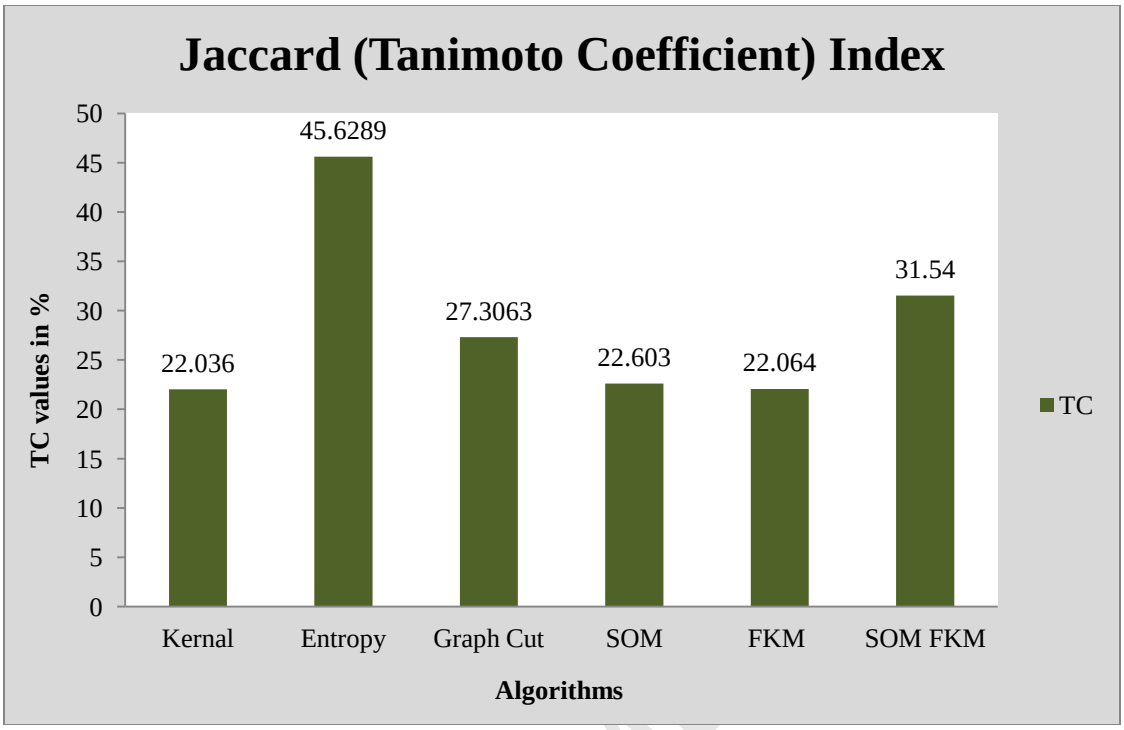

Fig. 25. Comparison of soft computing algorithms using TC values.

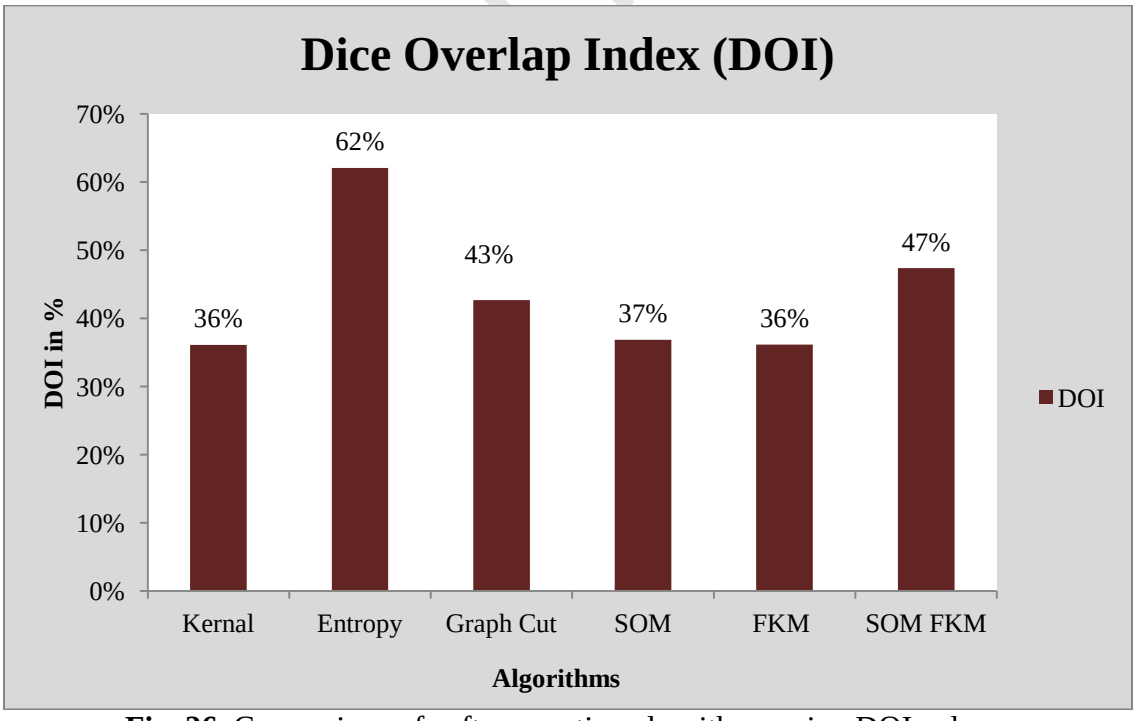

Fig. 26. Comparison of soft computing algorithms using DOI values.

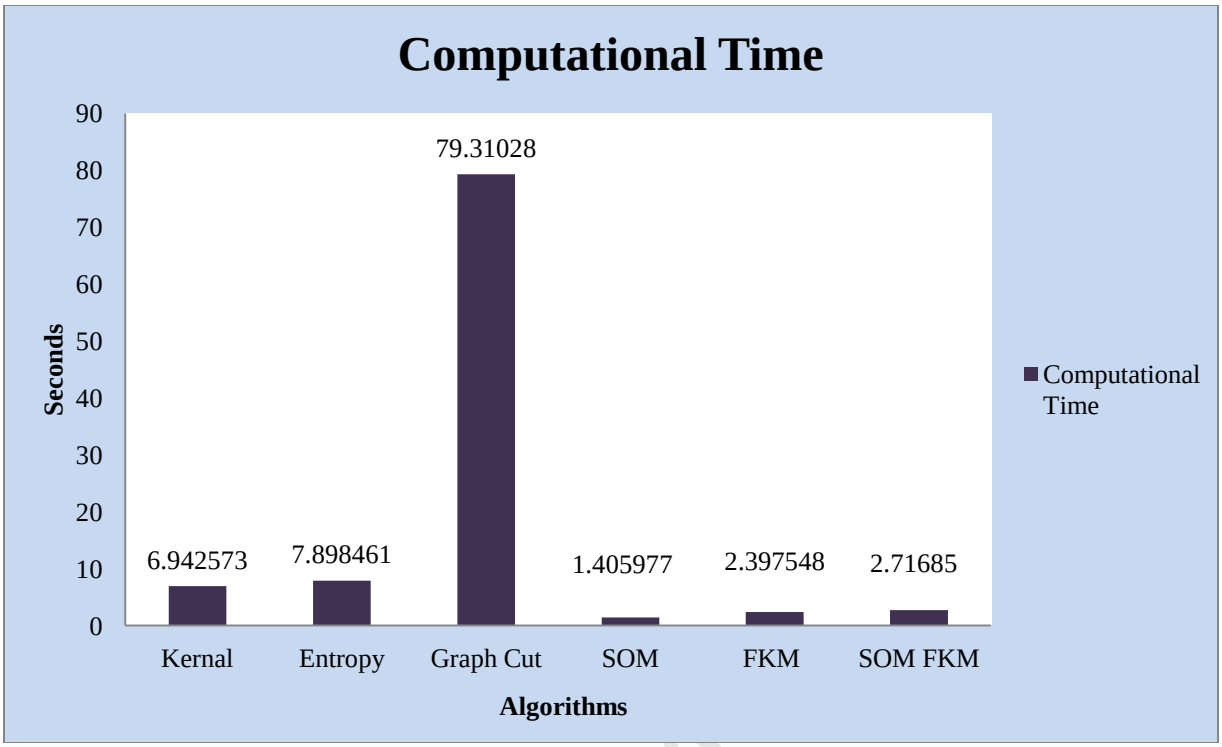

Fig. 27. Comparison of medical image segmentation algorithms using time duration.

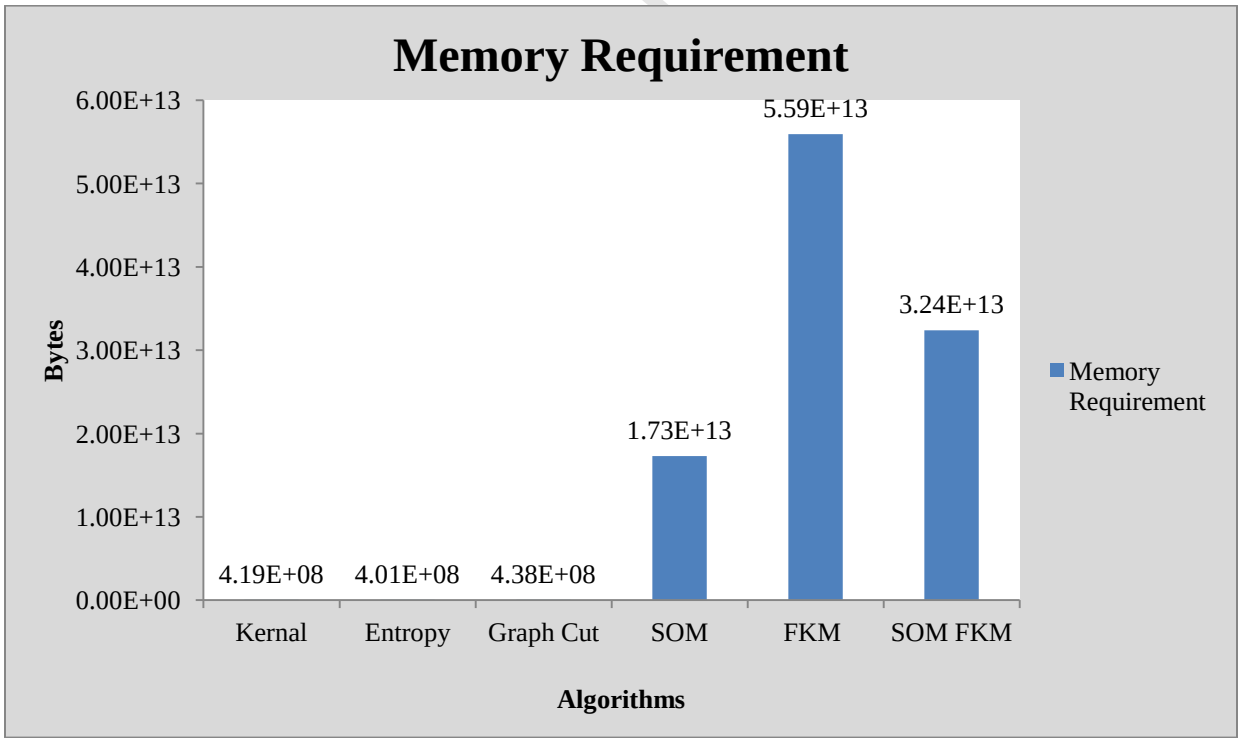

Fig. 28. Comparison of medical image segmentation algorithms using memory requirement.

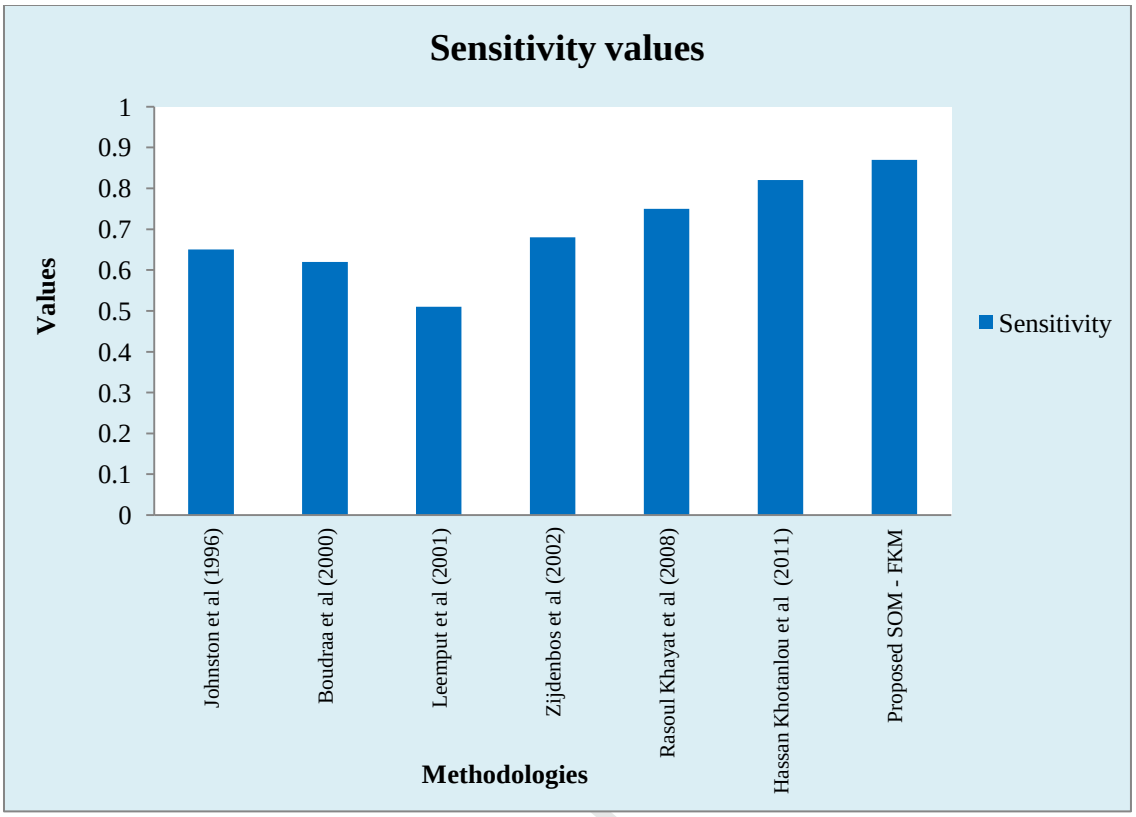

Fig. 29. Comparison of Sensitivity (or) Overlap Fraction values with other competitive algorithms.

Tables:

Images		MSE	PSNR	TC	DOI	Computational time	Memory Requirement
Clinical Datasets	1.	2.5571	44.0534	0.2012	0.3351	2.531207	2.4427e+013
	2.	3.4964	42.6946	0.3142	0.4781	2.166391	3.1064e+013
	3.	2.8866	43.5269	0.3176	0.4821	3.028439	1.9803e+013
	4.	2.8268	43.6178	0.2268	0.3698	5.128464	3.6144e+013
	5.	2.6551	43.8900	0.2052	0.3406	2.452931	3.1393e+013
	6.	2.2346	44.6388	0.2115	0.3491	3.729248	2.4774e+013
	7.	0.9899	48.1751	0.3335	0.5002	1.967794	3.7894e+013
	8.	2.2226	44.6622	0.2859	0.4447	2.125825	2.6166e+013
	9.	2.4823	44.1823	0.2130	0.3512	3.066892	4.3516e+013
	10.	1.8648	45.4244	0.3198	0.4846	2.403510	3.2310e+013
	11.	3.4029	42.8123	0.4152	0.5867	2.402933	2.8402e+013
	12.	2.5523	44.0615	0.2228	0.3644	3.685131	3.7398e+013
	13.	1.9620	5.2038	0.2182	0.3582	2.131511	4.1478e+013
	14.	1.9004	45.3423	0.2957	0.4564	1.924268	3.4124e+013
	15.	1.4354	46.5611	0.3359	0.5029	1.944054	4.0958e+013
	16.	1.7301	45.7502	0.2770	0.4338	1.465142	3.6330e+013
	17.	5.7986	40.4976	0.1982	0.3308	4.866730	3.1151e+013
Harvard images	18.	0.9830	48.2055	0.3759	0.5464	2.279997	2.3616e+013
	19.	1.8620	45.4309	0.3564	0.5255	3.245901	3.1409e+013
	20.	1.1874	47.3847	0.3178	0.4823	2.400932	3.2659e+013
	21.	2.1070	44.8941	0.3093	0.4724	1.572801	3.0744e+013
	22.	2.1285	44.8501	0.3341	0.5009	2.965126	3.3951e+013
	23.	0.8359	48.9094	0.3981	0.5695	2.779671	3.3601e+013
	24.	3.3151	42.9259	0.3894	0.5606	6.453621	3.6221e+013
	25.	1.6880	45.8572	0.3939	0.5652	1.684540	3.3825e+013
	26.	2.3832	44.3591	0.4273	0.5988	2.651933	3.7745e+013
	27.	2.3011	44.5114	0.3521	0.5208	1.708257	3.2618e+013
	28.	2.8465	43.5877	0.3478	0.5161	3.968782	3.6706e+013
	29.	1.9070	45.3274	0.4024	0.5739	2.839513	3.6674e+013
	30.	0.4625	1.4796	0.3851	0.5560	1.619065	3.6615e+013
	31.	2.7641	43.7153	0.3674	0.5373	4.361223	3.4649e+013
	32.	0.9855	48.1940	0.3981	0.5695	2.177429	3.3149e+013
	33.	0.8573	48.7995	0.4504	0.6211	1.715861	2.6559e+013
	34.	0.9316	8.4385	0.4189	0.5904	1.806791	2.8988e+013
	35.	1.4246	46.5939	0.4189	0.5904	3.309900	3.1353e+013
	36.	2.3401	44.4384	0.1968	0.3289	2.597943	3.6327e+013
	37.	2.9245	43.4703	0.1807	0.3060	2.393811	2.6458e+013
	38.	2.5364	44.0887	0.1760	0.2993	1.686739	2.0459e+013

Table 1 Performance evaluation for the proposed SOM based FKM Algorithm.

Algorithm	Similarity Criteria	Overlap Fraction	Extra Fraction	Specificity
FCM	0.7273	0.7500	0.3125	0.6875
Kernel based Fuzzy Clustering	0.7937	0.7576	0.1515	0.8214
Graph based Fuzzy Clustering	0.6897	0.6667	0.2667	0.6923
Entropy based Fuzzy Clustering	0.6429	0.5455	0.7619	0.1515
SOM	0.7119	0.6563	0.7600	0.1875
FKM	0.7742	0.7500	0.1875	0.7857
Proposed SOM - FKM	**0.9189**	**0.8718**	**0.0256**	**0.9737**

Table 2 Comparison of SI, OF, EF and Specificity values.